An overview of nuclear Quantum Monte Carlo

Università degli Studi Roma 3
Seminario di Fisica, February 25, 2020

Alessandro Lovato

Istituto Nazionale di Fisica Nucleare

Argonne NATIONAL LABORATORY

In collaboration with:
O. Benhar, J. Carlson, S. Gandolfi, N. Rocco, and R. Schiavilla

Introduction

Atomic nuclei are **strongly interacting many-body systems** exhibiting fascinating properties including: shell structure, pairing and superfluidity, deformation, and self-emerging clustering.

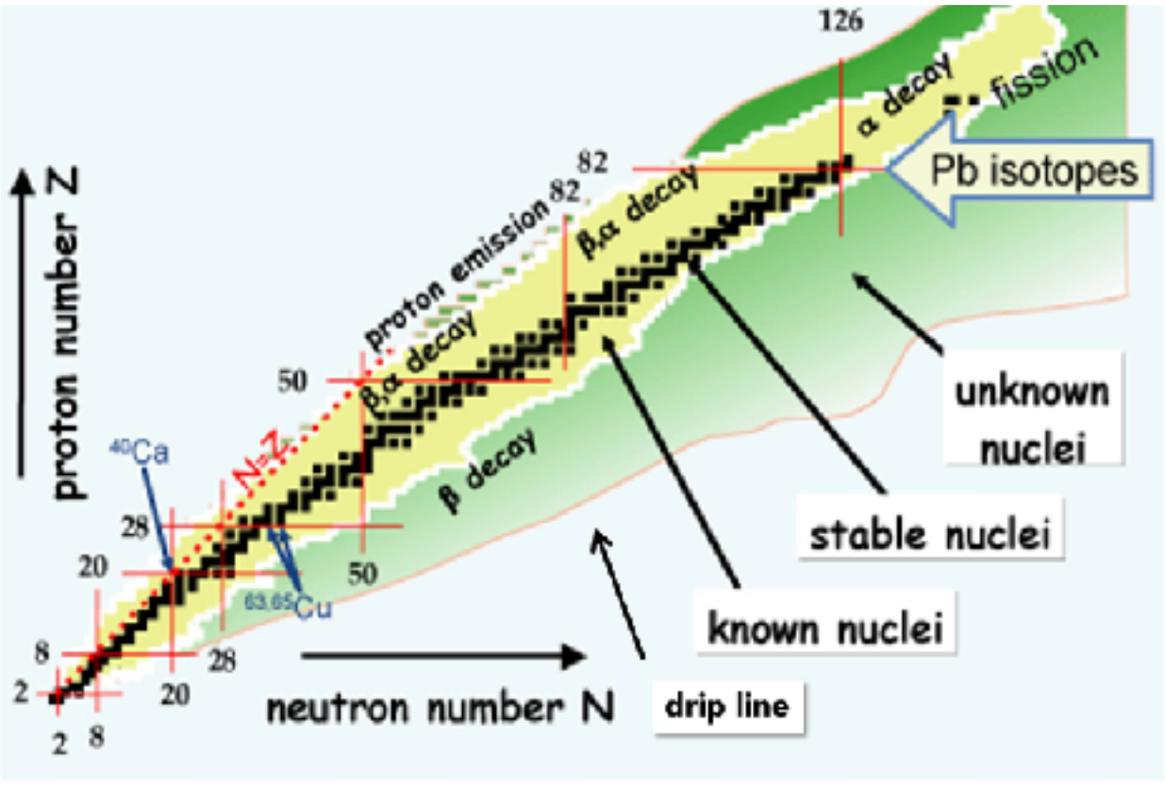

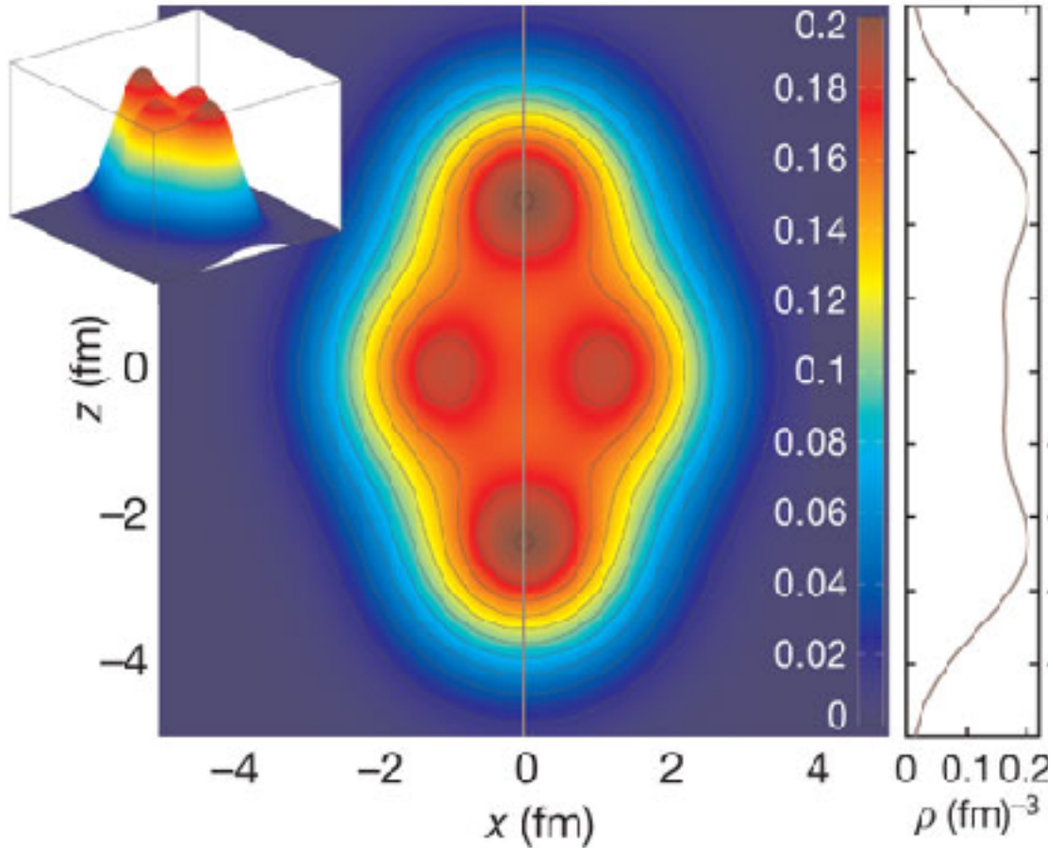

Understanding their **structure, reactions, and electroweak properties** within a unified framework well-rooted in quantum chromodynamics has been a long-standing goal of nuclear physics.

The microscopic model of nuclear theory

Effective Hamiltonians and consistent currents

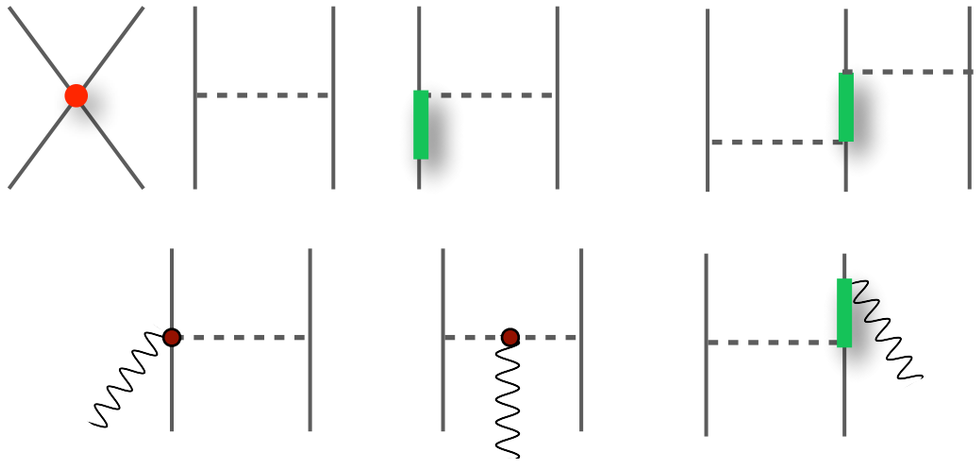

Accurate nuclear many-body methods

$$H|\Psi_n\rangle = E_n|\Psi_n\rangle$$

$$J_{mn} = \langle\Psi_m|J|\Psi_n\rangle$$

Quantum Chromodynamcs

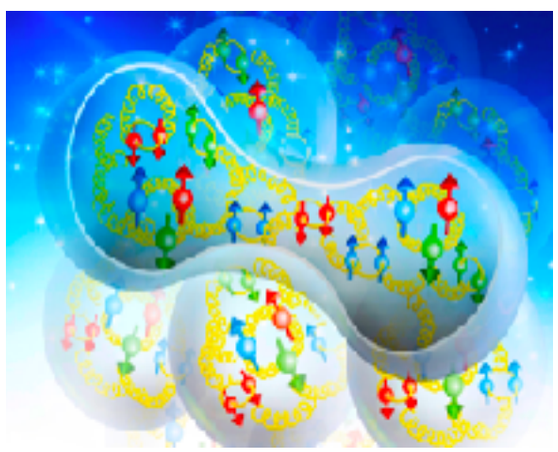

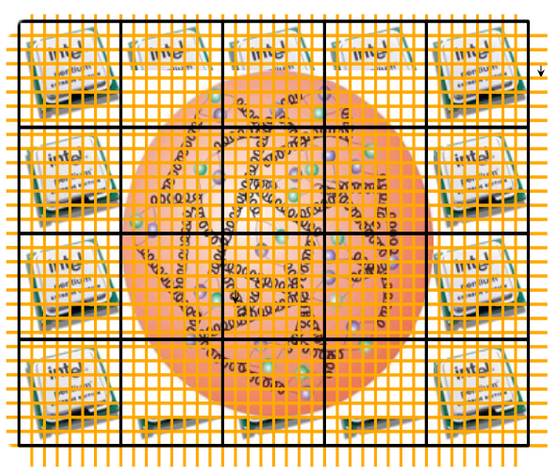

Atomic nuclei and neutrino scattering

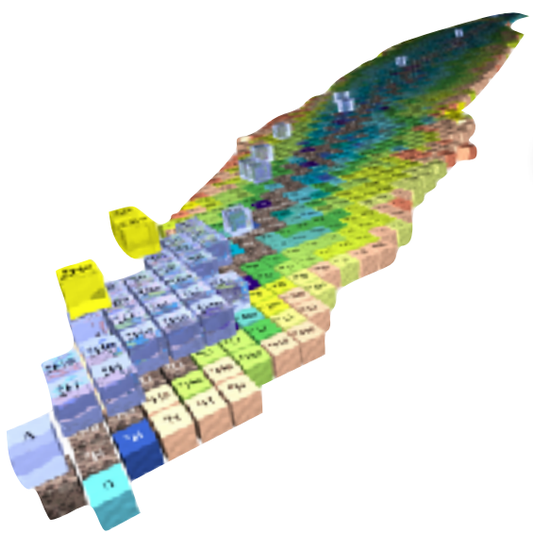

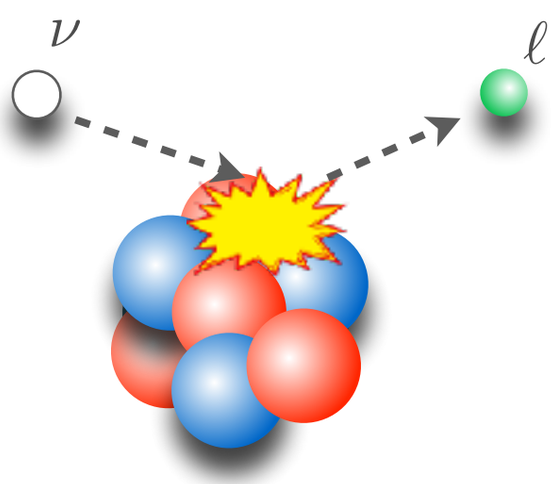

Hamiltonian and electroweak currents

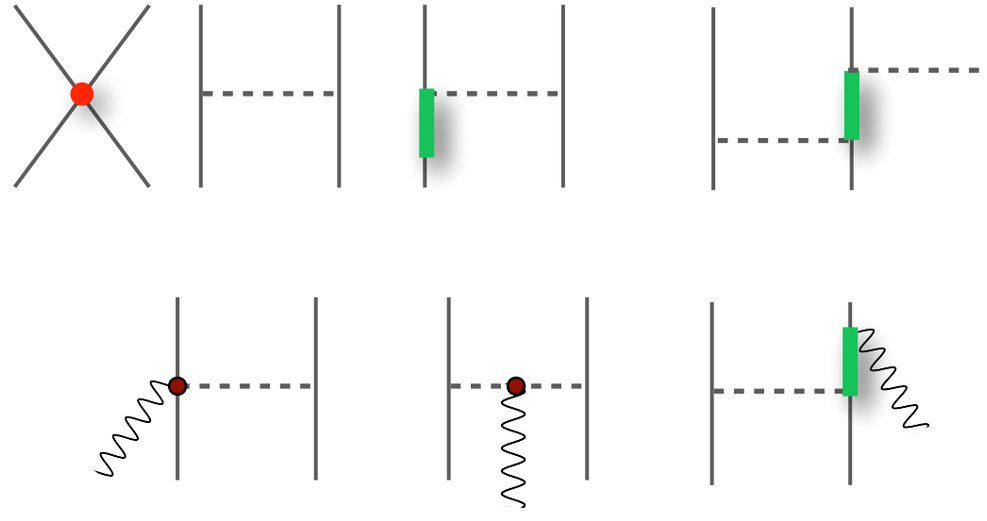

The microscopic model of nuclear theory

In the low-energy regime, **quark and gluons are confined within hadrons** and the relevant degrees of freedoms are protons, neutrons, and pions

Effective field theories are the link between QCD and nuclear observables. They exploit the separation between the “hard” (M~nucleon mass) and “soft” (Q ~ exchanged momentum) scales

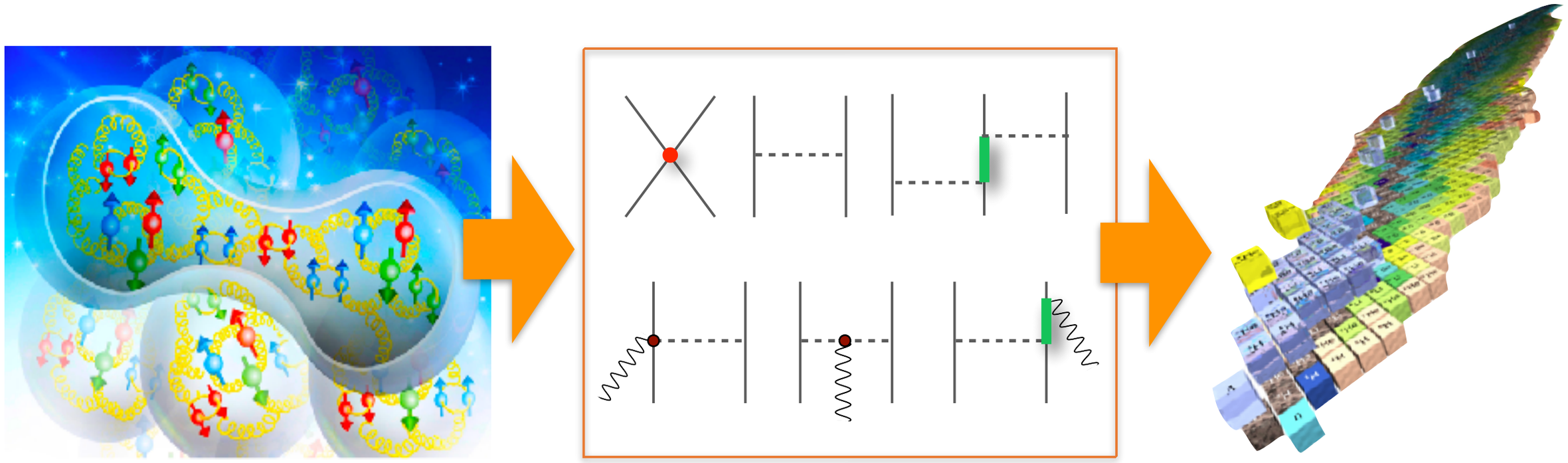

Nucleons can treated as point-like particles interacting through the Hamiltonian

$$H = \sum_i \frac{\mathbf{p}_i^2}{2m} + \sum_{i<j} v_{ij} + \sum_{i<j<k} V_{ijk} + \dots$$

Two-body (phenomenological) potential

Realistic local, configuration-space potential are controlled by **thousands np and pp scattering data** below 350 MeV of the Nijmegen and Granada databases

Nuclear potentials are strongly spin-isospin dependent. **Argonne v_{18}** can be written as

$$v_{18}(r_{ij}) = v_{ij}^{\gamma} + v_{ij}^{\pi} + v_{ij}^{I} + v_{ij}^{S} = \sum_{p=1}^{18} v^{p}(r_{ij}) O_{ij}^{p}$$

- Static part $O_{ij}^{p=1-6} = (1, \sigma_{ij}, S_{ij}) \otimes (1, \tau_{ij})$
- Spin-orbit $O_{ij}^{p=7-8} = \mathbf{L}_{ij} \cdot \mathbf{S}_{ij} \otimes (1, \tau_{ij})$

Some of the Feynman diagrams effectively included in the Argonne potential

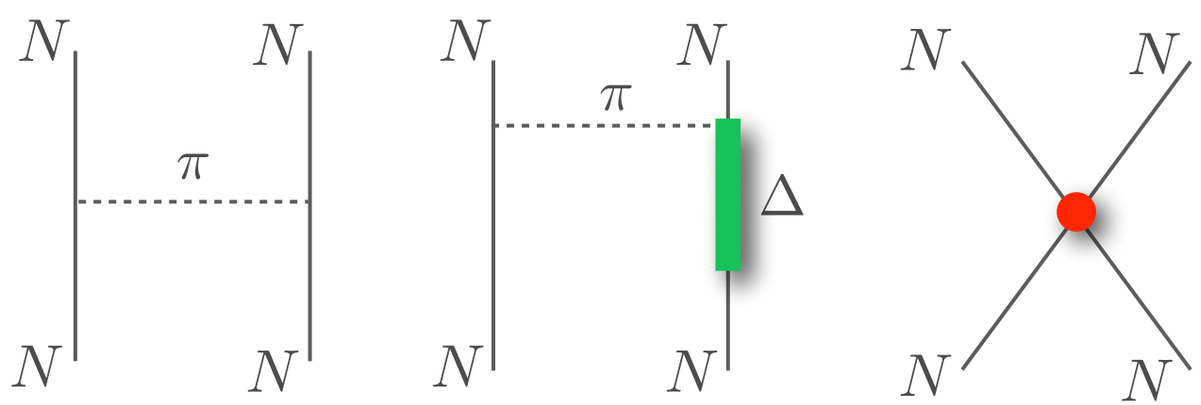

Three-body (phenomenological) potentials

An Hamiltonian which only includes Argonne v_{18} does not provide enough binding in the light nuclei and overestimates the equilibrium density of symmetric nuclear matter.

Nuclear three-body interactions are analogous to tidal forces: the gravitational force on the Earth is not just the sum of Earth-Moon and Earth-Sun forces

Illinois 7 contains: a two-pion exchange interaction, a phenomenological repulsive term, a two-pion S-wave contribution, and three-pion exchange diagrams.

$$V_{ijk} = V_{ijk}^{2\pi,P} + V_{ijk}^{2\pi,S} + V_{ijk}^{3\pi,\Delta R} + V_{ijk}^{R}$$

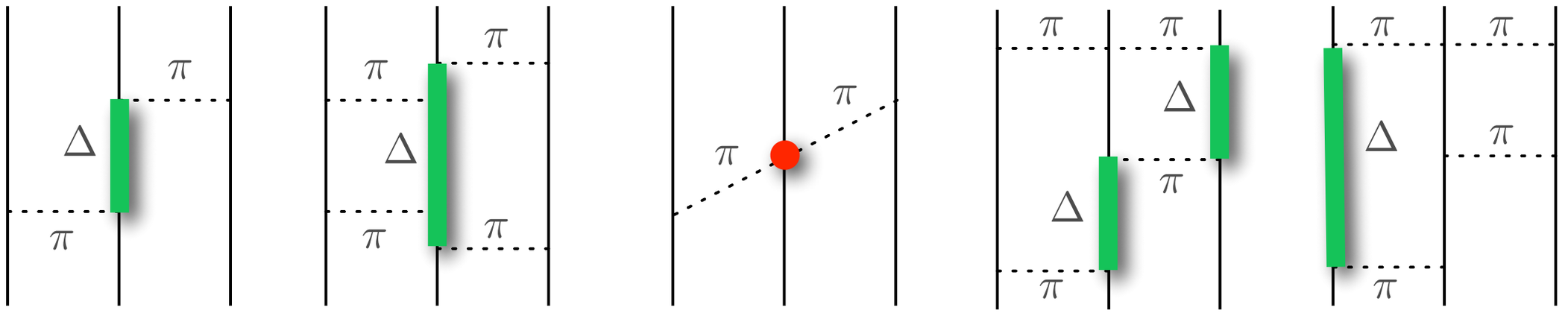

S. Pieper et al., PRC **64**, 014001 (2001)

The parameters of the hamiltonian are fit to properties of **exactly solvable light nuclear systems**.

Electroweak currents

The electromagnetic current is constrained by the Hamiltonian through the **continuity equation**

$$\boldsymbol{\nabla} \cdot \mathbf{J}_{\rm EM} + i[H, J^0_{\rm EM}] = 0$$

• The above equation implies that $\mathbf{J}_{\rm EM}$ involves two-nucleon contributions.

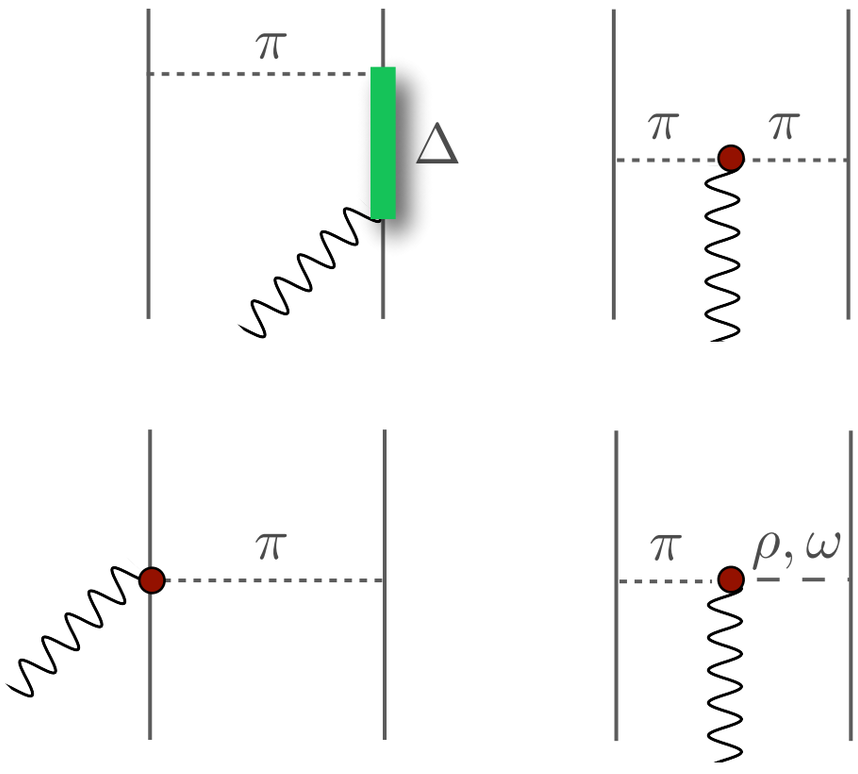

R. Schiavilla et al., PRC **45**, 2628 (1992)

L. Marcucci et al., PRC **72**, 014001 (2005)

• They are essential for low-momentum and low-energy transfer transitions.

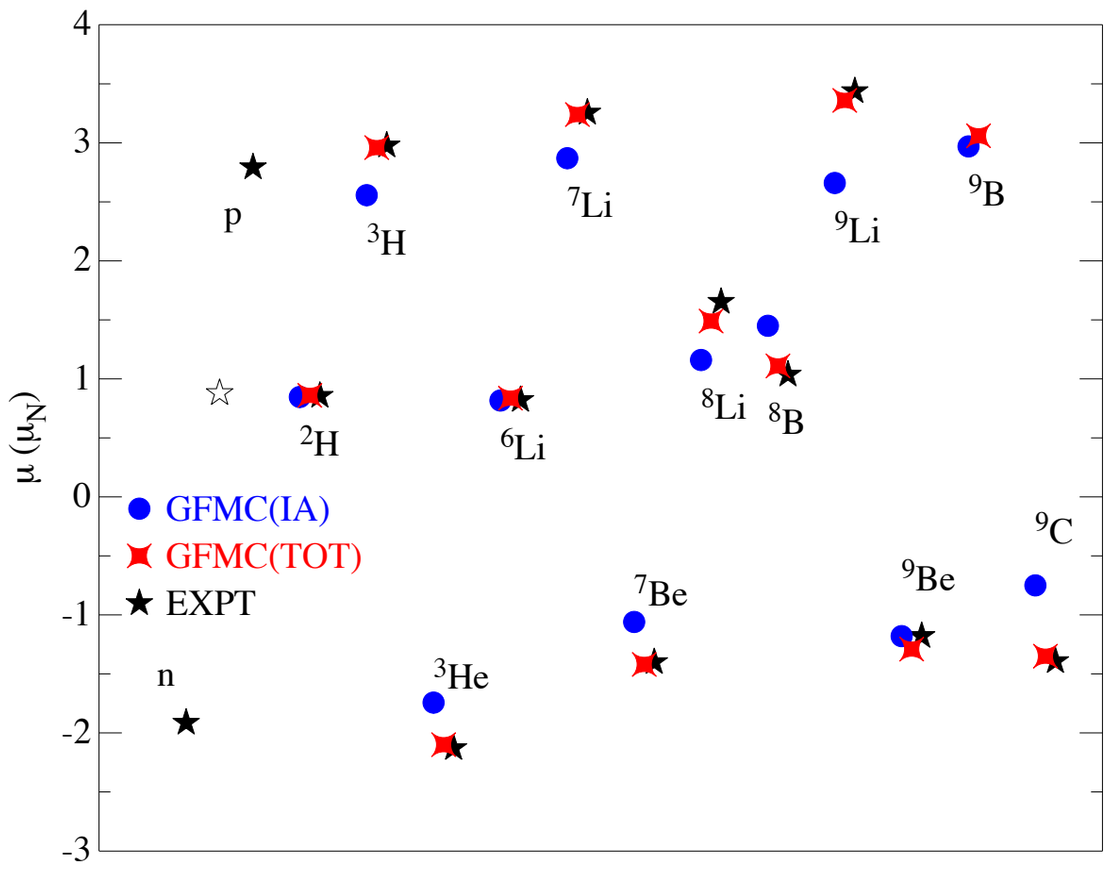

S. Pastore at al., PRC **87**, 035503 (2013)

Axial form factor

The axial one- and two-body currents are proportional to the **nucleon axial form factor**

A dipole ansatz fits the available deuteron-scattering data

$$G_A(Q^2) = \frac{g_A}{(1 + Q^2/M_A^2)^2}$$

More flexible parameterizations, based on the “z-expansion” have been recently proposed

Lattice-QCD calculations started becoming available.

T. Bhattacharya at al., PoS (LATTICE2019)

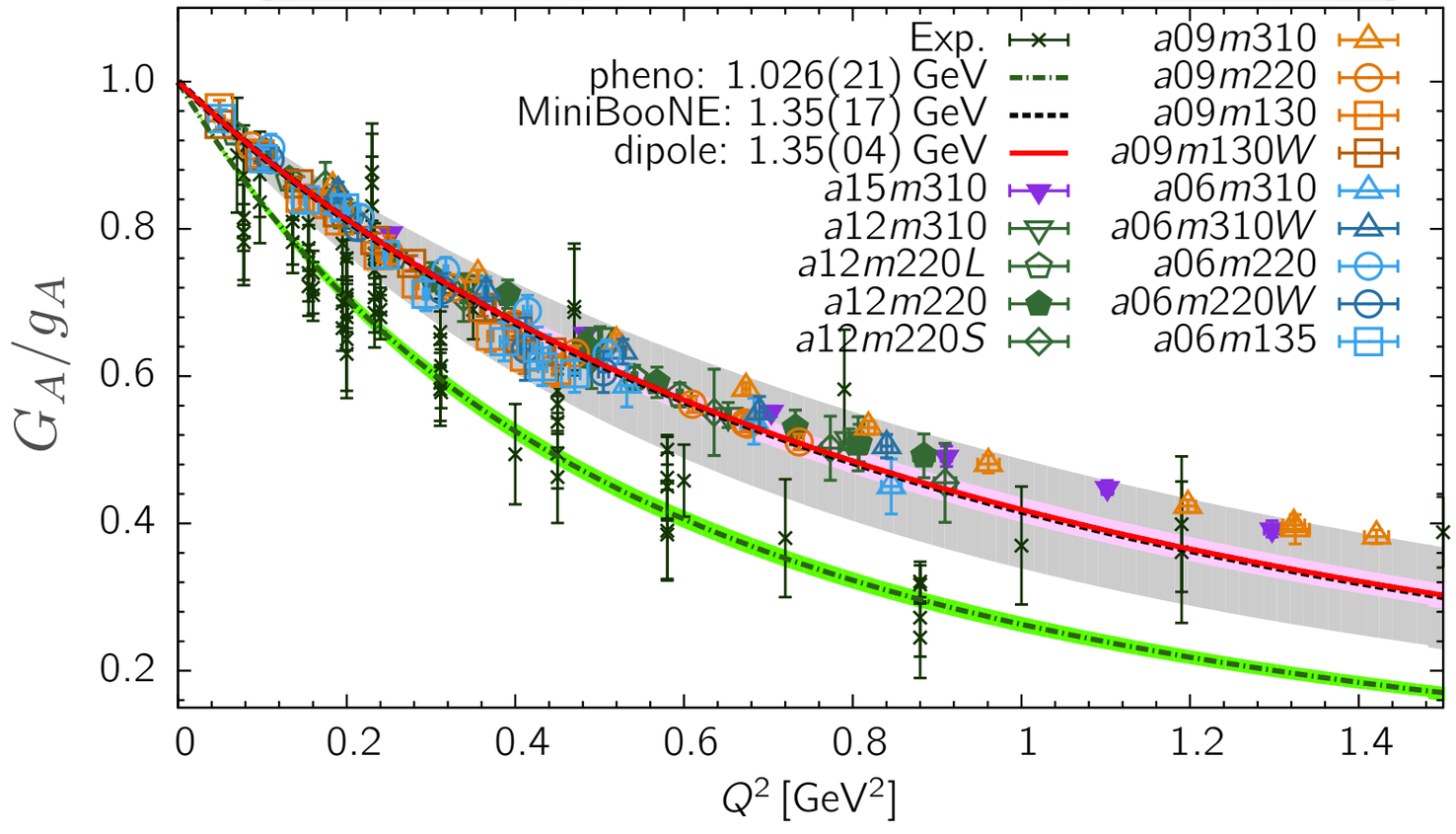

Accurate nuclear many-body methods

$$H|\Psi_n\rangle = E_n|\Psi_n\rangle$$

$$J_{mn} = \langle\Psi_m|J|\Psi_n\rangle$$

Variational Monte Carlo

In variational Monte Carlo, one **assumes a suitable form for the trial wave function**

$$\Psi_T = \left(1 + \sum_{i<j<k} F_{ijk}\right)\left(\mathcal{S}\prod_{i<j} F_{ij}\right)\Phi_A(J, M, T_z)$$

The best variational parameters are found by **optimizing the variational energy**

$$E_T = \langle \Psi_T | H | \Psi_T \rangle \geq E_0$$

The long-range antisymmetric Φ_A is typically a Slater determinant of single-particle orbitals

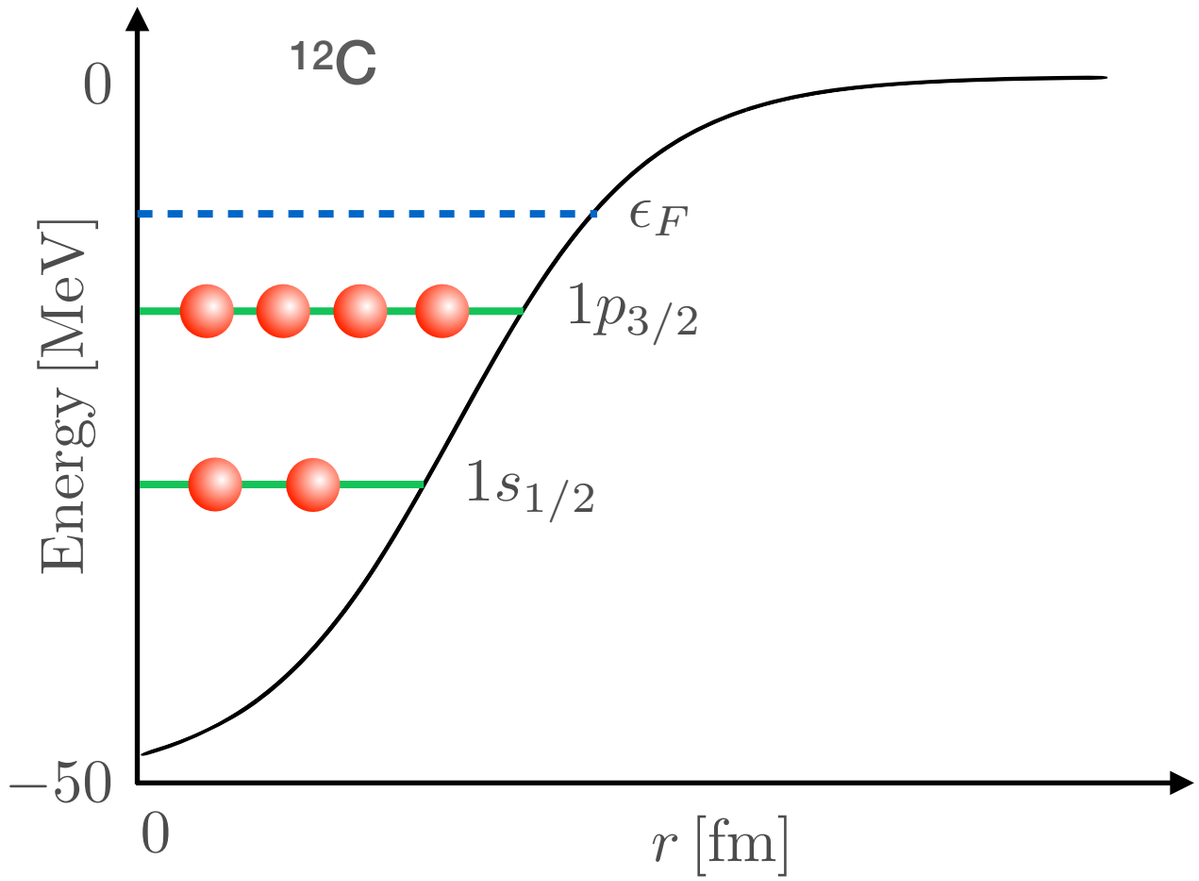

Variational Monte Carlo

In variational Monte Carlo, one **assumes a suitable form for the trial wave function**

$$\Psi_T = \left(1 + \sum_{i<j<k} F_{ijk}\right)\left(\mathcal{S}\prod_{i<j} F_{ij}\right)\Phi_A(J, M, T_z)$$

The best variational parameters are found by **optimizing the variational energy**

$$E_T = \langle \Psi_T | H | \Psi_T \rangle \geq E_0$$

The correlation operator reflects the spin-isospin dependence of the nuclear interaction

$$F_{ij} \simeq \sum_p f^p(r_{ij}) O^p_{ij} \qquad F_{ijk} = \sum_x \epsilon_x V^x_{ijk}(\tilde{r}_{ij}, \tilde{r}_{ik}, \tilde{r}_{jk})$$

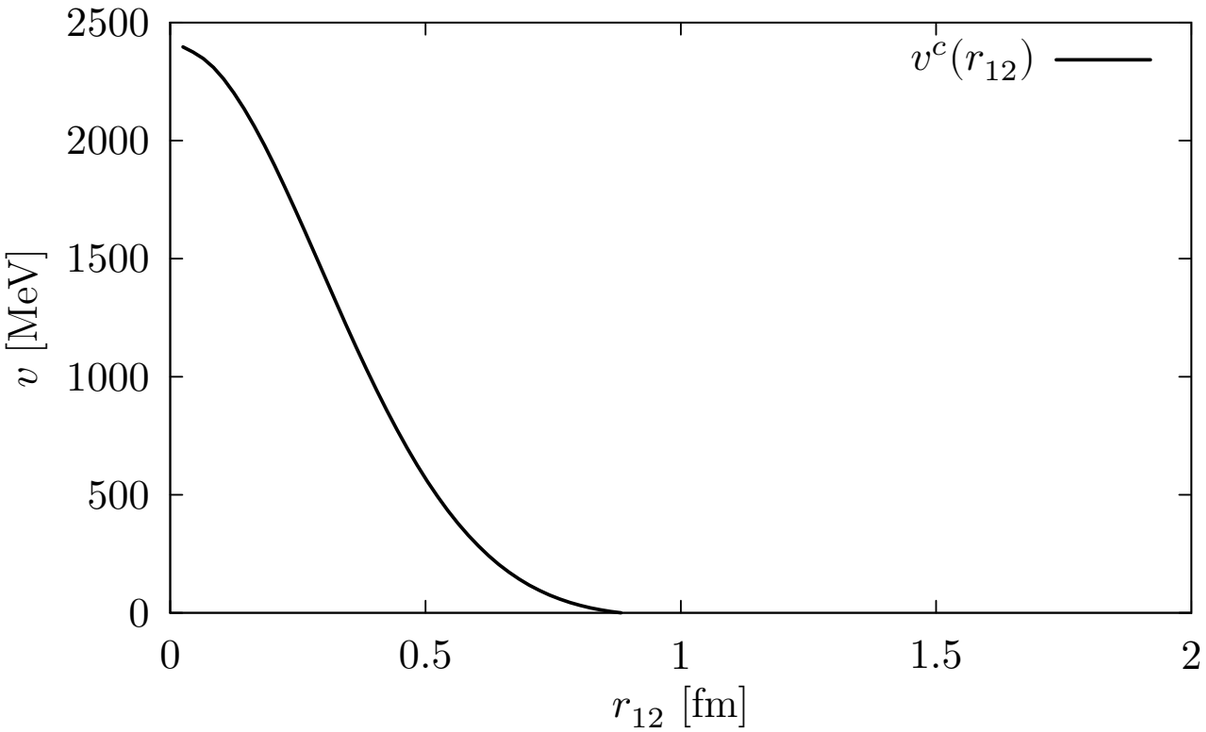

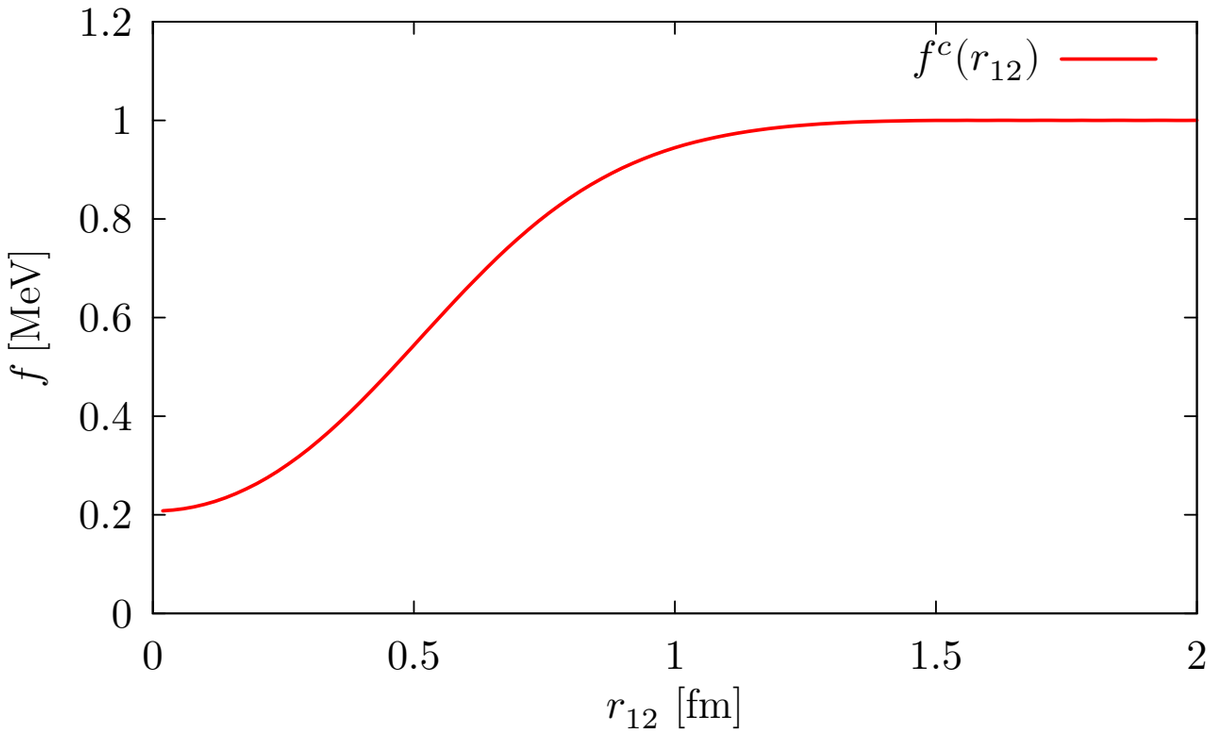

Green's function Monte Carlo

GFMC **overcomes the limitations of the variational wave-function** by using an imaginary-time projection technique

Any trial wave function can be expanded in the complete set of eigenstates of the the Hamiltonian according to

$$|\Psi_T\rangle = \sum_n c_n |\Psi_n\rangle \qquad\qquad H|\Psi_n\rangle = E_n|\Psi_n\rangle$$

GFMC **projects out the exact lowest-energy state**, provided the trial wave function it is not orthogonal to the ground state.

$$\lim_{\tau\to\infty} e^{-(H-E_0)\tau}|\Psi_T\rangle =$$

$$\lim_{\tau\to\infty} \sum_n c_n\, e^{-(E_n-E_0)\tau}|\Psi_n\rangle = c_0|\Psi_0\rangle$$

B. Pudliner et al., PRC **56**, 1720 (1997)

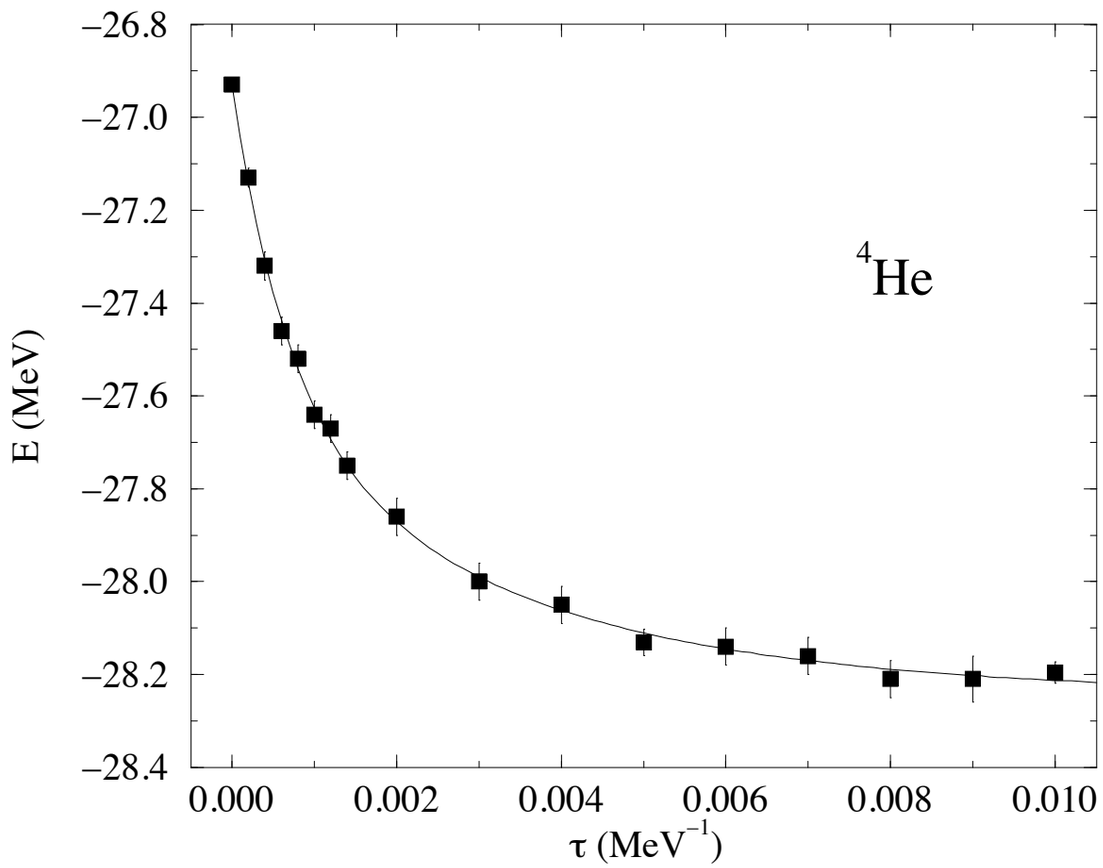

Green's function Monte Carlo

The imaginary-time evolution is broken into N small imaginary-time steps

$$\langle X_N|\Psi(\tau)\rangle = \prod_{I=1}^{N-1} \int dX_i \langle X_N|e^{-(H-E_0)\delta\tau}|X_{N-1}\rangle \dots \langle X_2|e^{-(H-E_0)\delta\tau}|X_1\rangle\langle X_1|\Psi_T\rangle$$

The generalized coordinate denotes both positions and spin-isospin of the nucleons

$$|X\rangle \longleftrightarrow |R,S\rangle$$

The **short-time propagator** factorizes as

$$\langle X'|e^{-(H-E_0)\delta\tau}|X\rangle \simeq \langle X'|e^{-T\delta\tau}e^{-(V-E_0)\delta\tau}|X\rangle$$

The kinetic energy describes the **Brownian diffusion** of A particles

$$\langle X|e^{-T\delta\tau}|X'\rangle = \left(\frac{m}{2\pi\delta\tau}\right)^{\frac{3A}{2}} e^{-\frac{m(R-R')^2}{2\delta\tau}} \delta(S-S')$$

Putting aside its spin-dependent components the potential is included in the weight of the configuration

$$\langle X'|e^{-(V-E_0)\delta\tau}|X\rangle = e^{-[V(X)-E_0]\delta\tau}\delta(X-X')$$

Green's function Monte Carlo

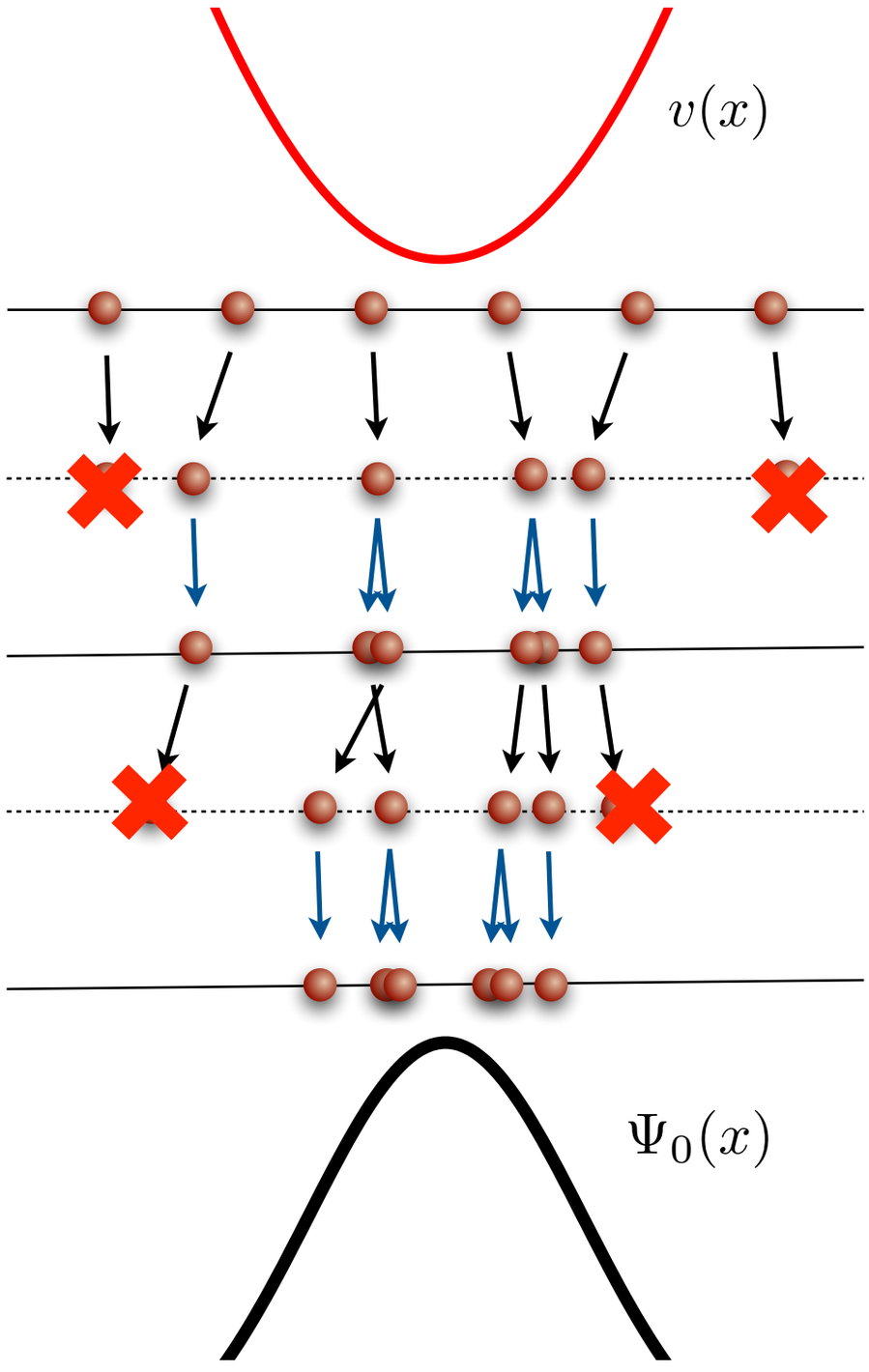

- A set of walkers is sampled from the trial wave function

- Gaussian drift for the kinetic energy

$$\left(\frac{m}{2\pi\hbar^2\Delta\tau}\right)^{\frac{1}{2}} e^{-\frac{m}{2\hbar^2\Delta\tau}(x_i - x_{i+1})^2}$$

- Branching and killing of the walkers induced by the potential weight

$$w(x_{i+1}) = e^{-[V(x_{i+1}) - E_0]\Delta\tau}$$

- Ground-state expectation values are estimated during the diffusion

$$\langle H \rangle = \frac{\sum_{x_i} \langle x_i | H | \Psi_T \rangle w(x_i)}{\sum_{x_i} \langle x_i | \Psi_T \rangle w(x_i)}$$

One-dimensional harmonic oscillator

$$H = -\frac{1}{2}\frac{d^2}{dx^2} + \frac{x^2}{2} \quad \longleftrightarrow \quad \Psi_0(x) = e^{-x^2/2}, \quad E_0 = 1/2$$

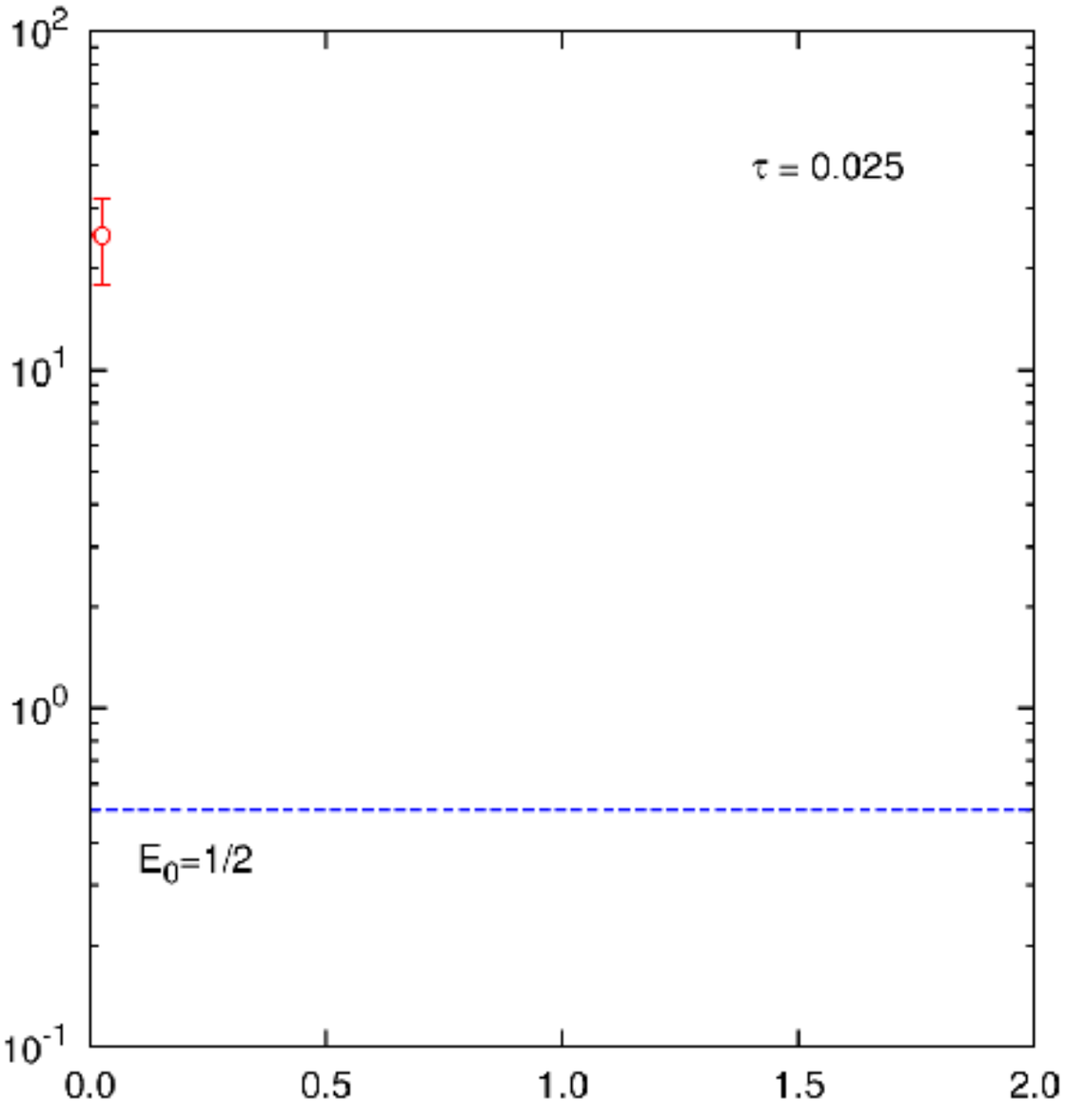

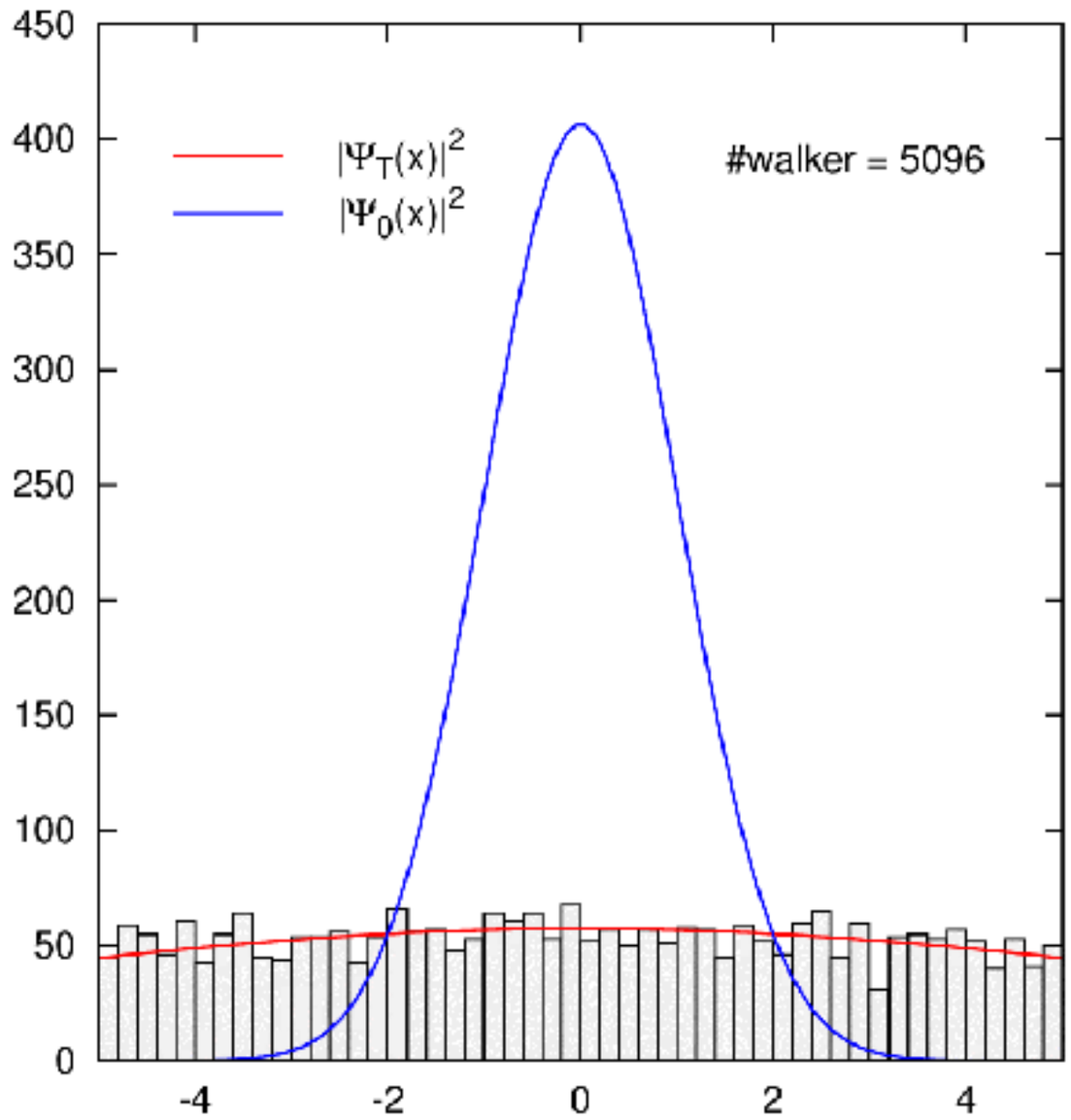

Green's function Monte Carlo

In the GFMC, **a sum over all the many-body spin-isospin states** is performed

$$\sum_{SS'}\langle S'|e^{-[V-E_0]\delta\tau}|S\rangle \simeq \sum_{SS'}\langle S'|\prod_{i<j}e^{-V_{ij}\delta\tau}|S\rangle e^{E_0\delta\tau}$$

Many-body spin-isospin states are utilized → unfavorable exponential scaling

The size of the spin state alone grows like 2^A

$$|S\rangle = \begin{pmatrix} s_{\uparrow\uparrow\uparrow} \\ s_{\uparrow\uparrow\downarrow} \\ s_{\uparrow\downarrow\uparrow} \\ s_{\uparrow\downarrow\downarrow} \\ s_{\downarrow\uparrow\uparrow} \\ s_{\downarrow\uparrow\downarrow} \\ s_{\downarrow\downarrow\uparrow} \\ s_{\downarrow\downarrow\downarrow} \end{pmatrix}$$

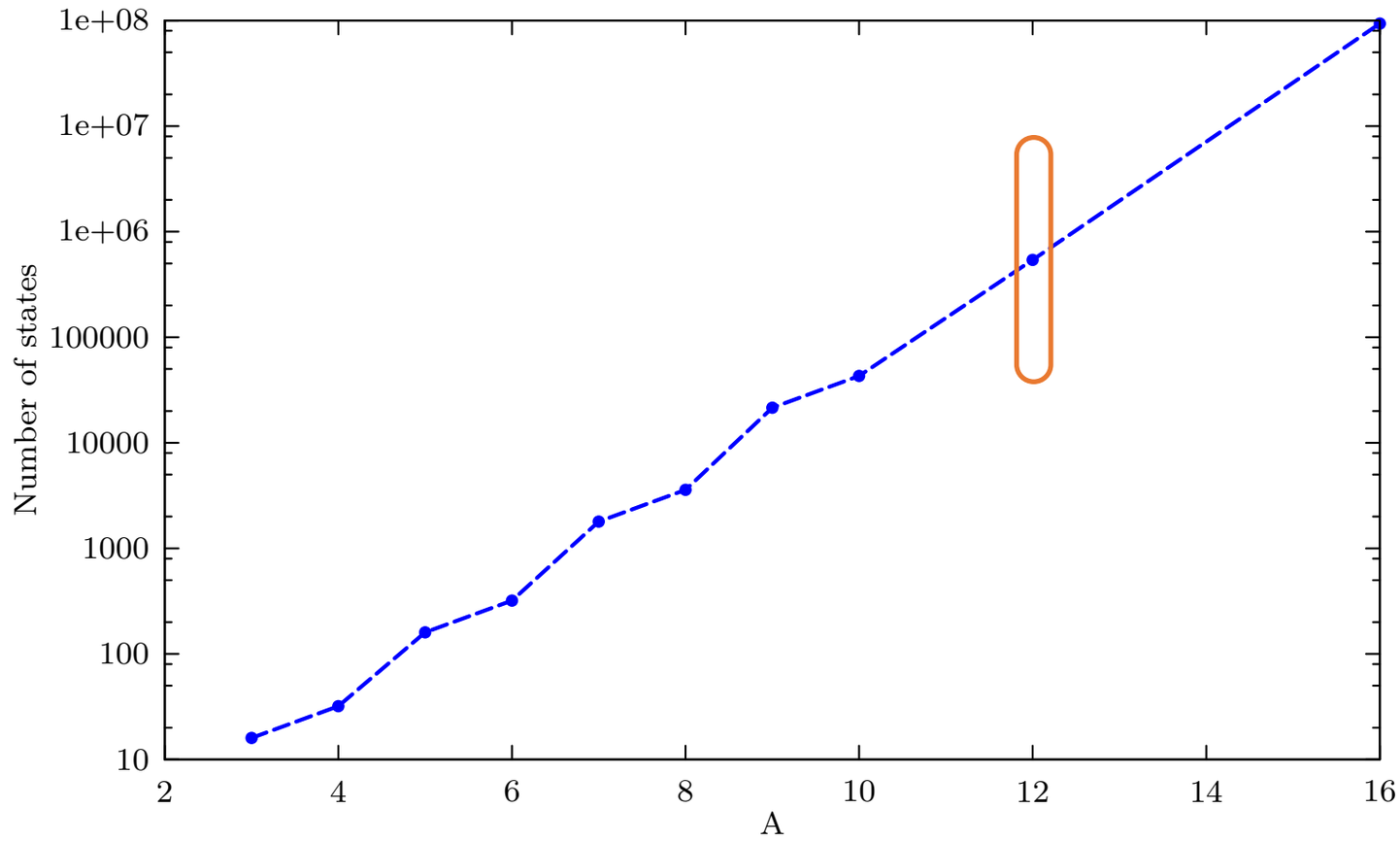

GFMC is extremely accurate but **limited to A=12 nuclei** and small (A ≤14) neutron systems

Importance-sampling and sign problem

The efficiency of the diffusion algorithm is crucially improved by the **importance sampling**

$$\langle X'|e^{-(H-E_0)\delta\tau}|X\rangle \longrightarrow \langle X'|e^{-(H-E_0)\delta\tau}|X\rangle \frac{\Psi_I(X')}{\Psi_I(X)}$$

Diffusion Monte Carlo algorithms suffers from the **fermion sign problem**, due to the fact that the importance-sampling wave-function entails components from the Bosonic ground-state

To alleviate it, in the AFDMC we implement an algorithm similar to the constrained-path approximation, but applicable to complex wave functions and propagators.

$$\frac{\Psi_I(R',S')}{\Psi_I(R,S)} \longrightarrow \max\left(\mathrm{Re}\left\{\frac{\Psi_T(R',S')}{\Psi_T(R,S)}\right\},0\right)$$

S. Zhang et al., PRB **55**, 7464 (1997)

The solution obtained from the constrained propagation is not the a rigorous upper-bound to the true ground-state energy

To remove the bias, the configurations obtained from a constrained propagation are further evolved using the following positive-definite importance sampling function

$$\Psi_G(X) = \sqrt{\mathrm{Re}\{\Psi_T(X)\}^2 + \alpha\,\mathrm{Im}\{\Psi_T(X)\}^2}$$

F. Pederiva et al., NPA, **742**, 255 (2004)

Exploiting leadership-class computers

GFMC has steadily undergone development to take advantage of each new generation of parallel machine and was one of the first to deliver new scientific results each time.

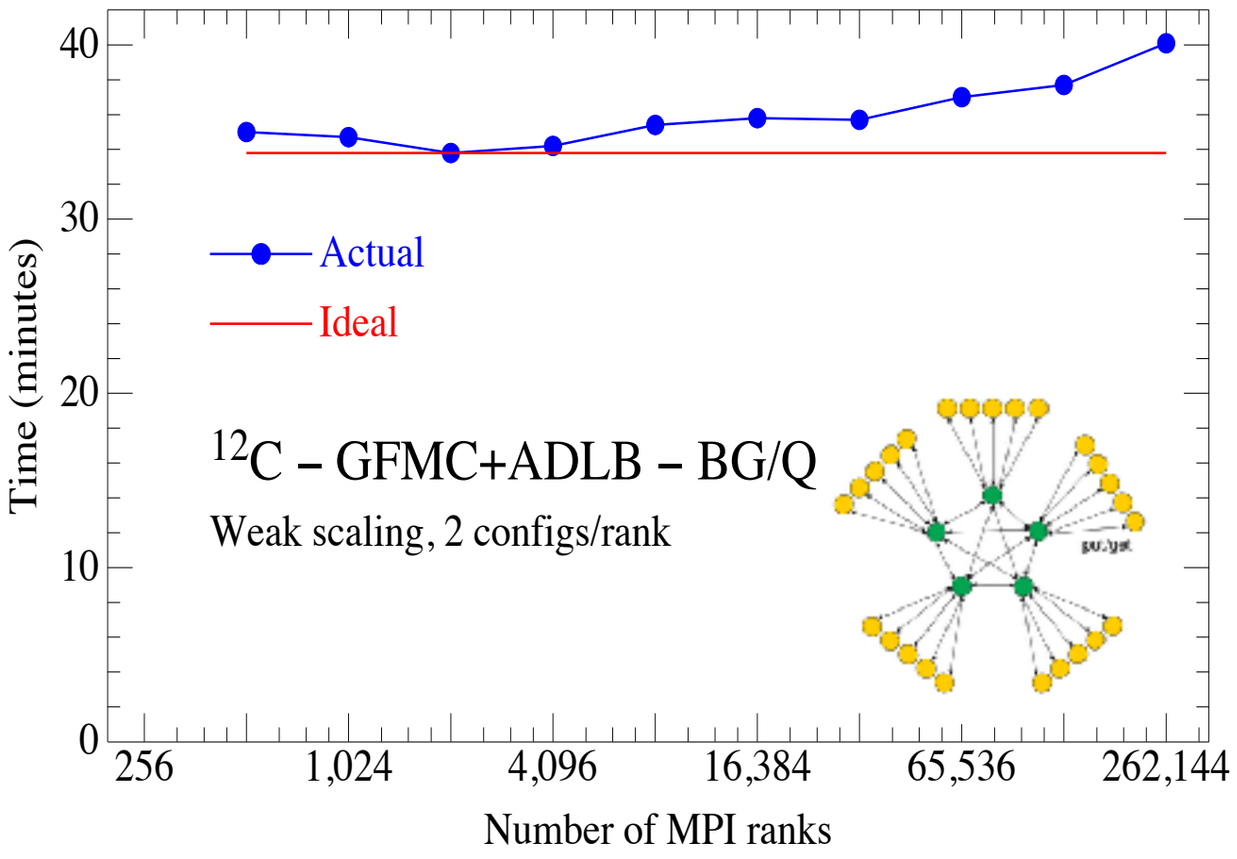

U.S. DEPARTMENT OF ENERGY
INCITE
LEADERSHIP COMPUTING

SciDAC
Scientific Discovery through Advanced Computing

Nuclear quantum Monte Carlo

Green's function Monte Carlo is suitable to **solve A ≤ 12 nuclei with ~1% accuracy**

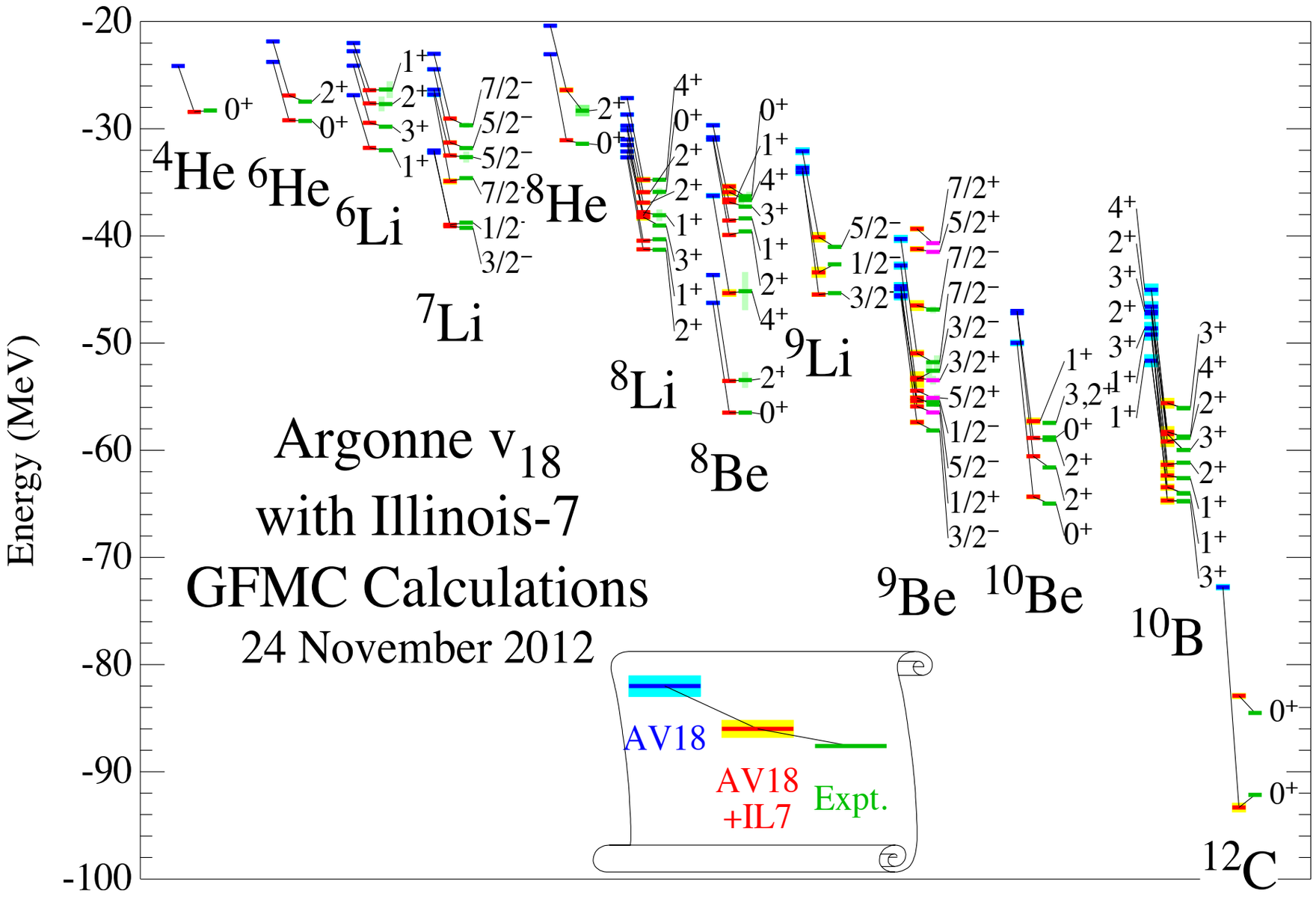

J. Carlson et al. RMP **87**, 1067 (2015)

Boron Radii

B. Maaß et al., PRL **122**, 182501 (2019)

Atomic physics:

- Accurate measurement of the isotope shift in the atomic transition ($2s^2\ 2p^2\ P_{1/2} \rightarrow 2s^2\ 3s^2\ S_{1/2}$)
- Ab-initio QED mass-shift calculations for five-electron systems

Nuclear theorists:

- We made GFMC calculations of point nucleon radii using the AV18+IL7 potentials
- No-core shell model calculations were made for chiral-EFT additional Hamiltonians
- Charge radii are evaluated by folding in the proton and neutron intrinsic radii along with the relativistic Darwin-Foldy correction

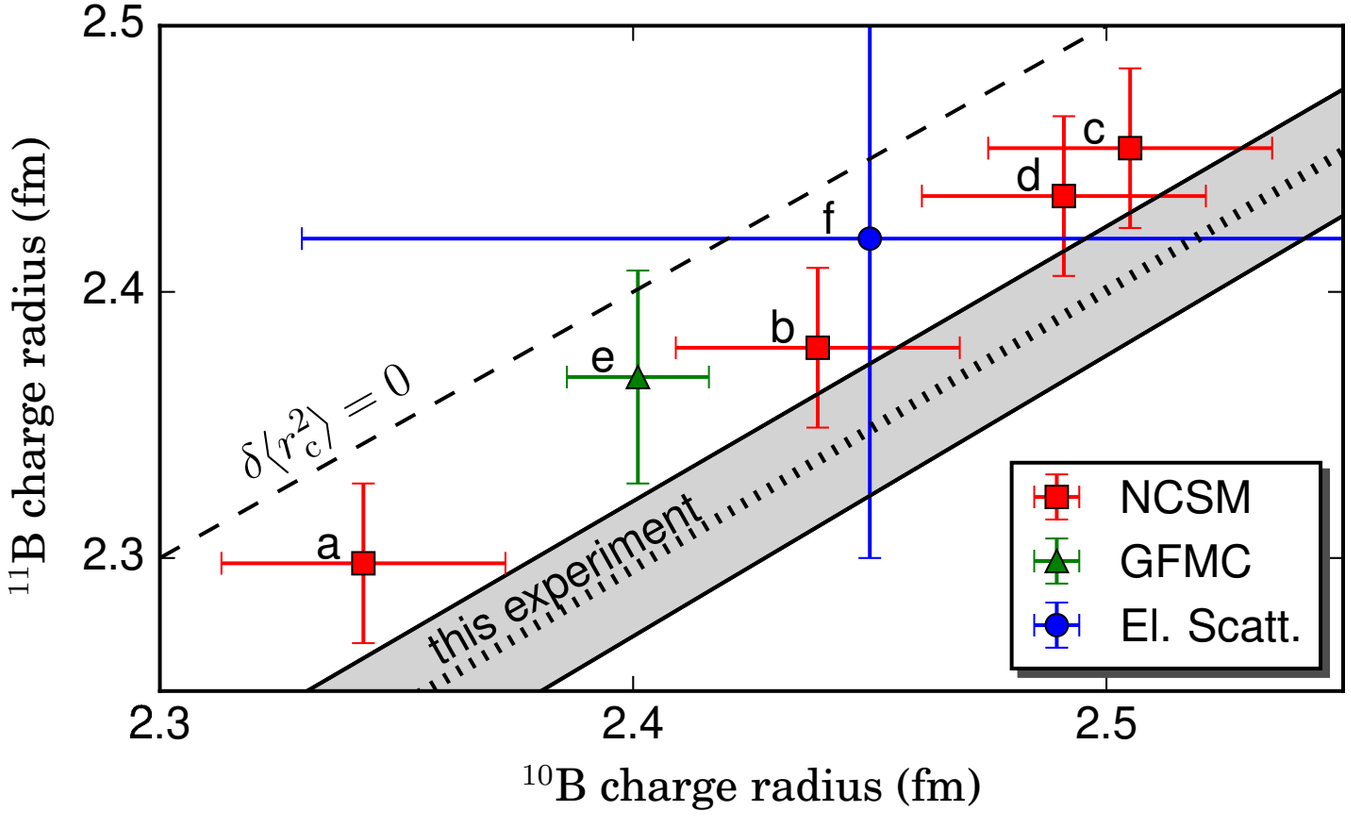

The experiment and nuclear theory results all agree that **^{11}B has the smaller charge radius**, although the theoretical values are systematically above the experiment by about one standard deviation.

The *basic model* of nuclear Physics

Impressive progress have been made within **coupled-cluster** and nuclear many-body techniques based on a basis expansion

The long-standing discrepancy between experimental and theoretical and experimental β-decay rates has been resolved from first principles calculations

P. Gysbers et al., Nature Phys. **15** 428-431 (2019)

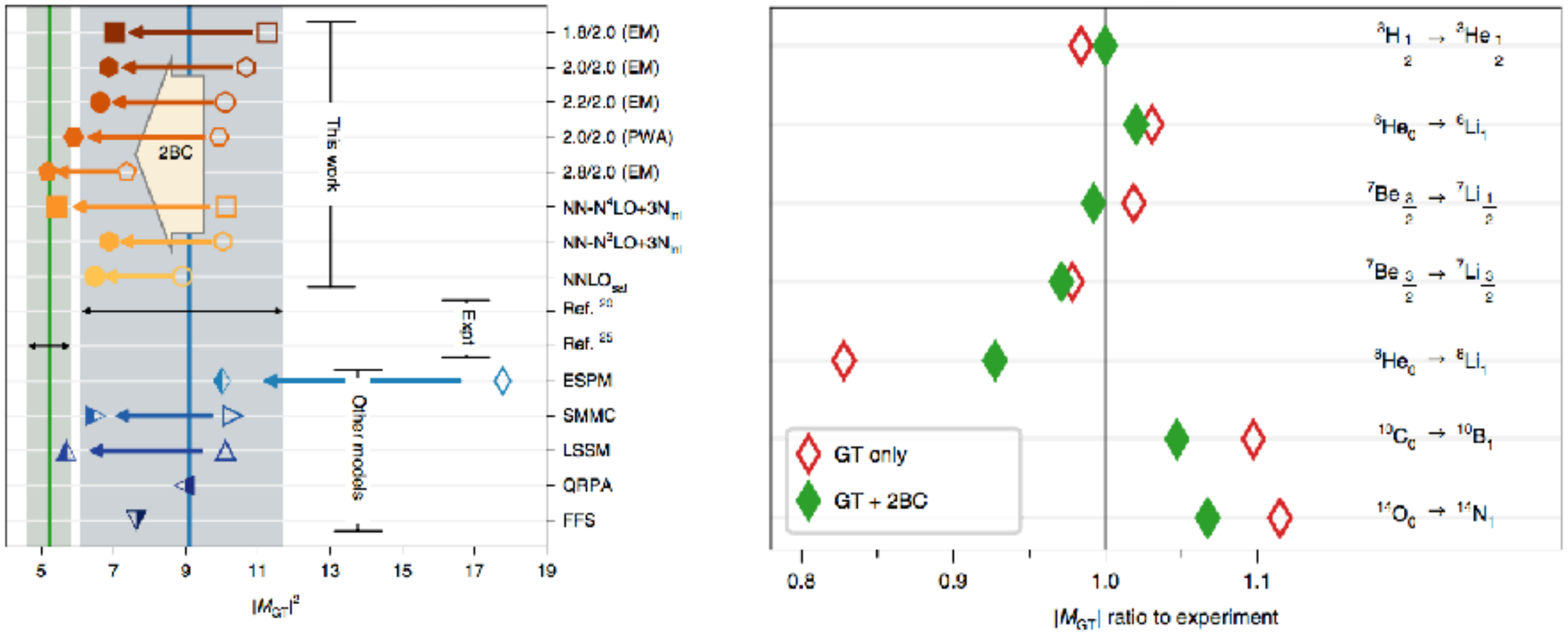

Quantum Monte Carlo remains the tool of choice to **simultaneously describe long-range structure and short-range dynamics** of atomic nuclei.

Neutrino-nucleus interaction

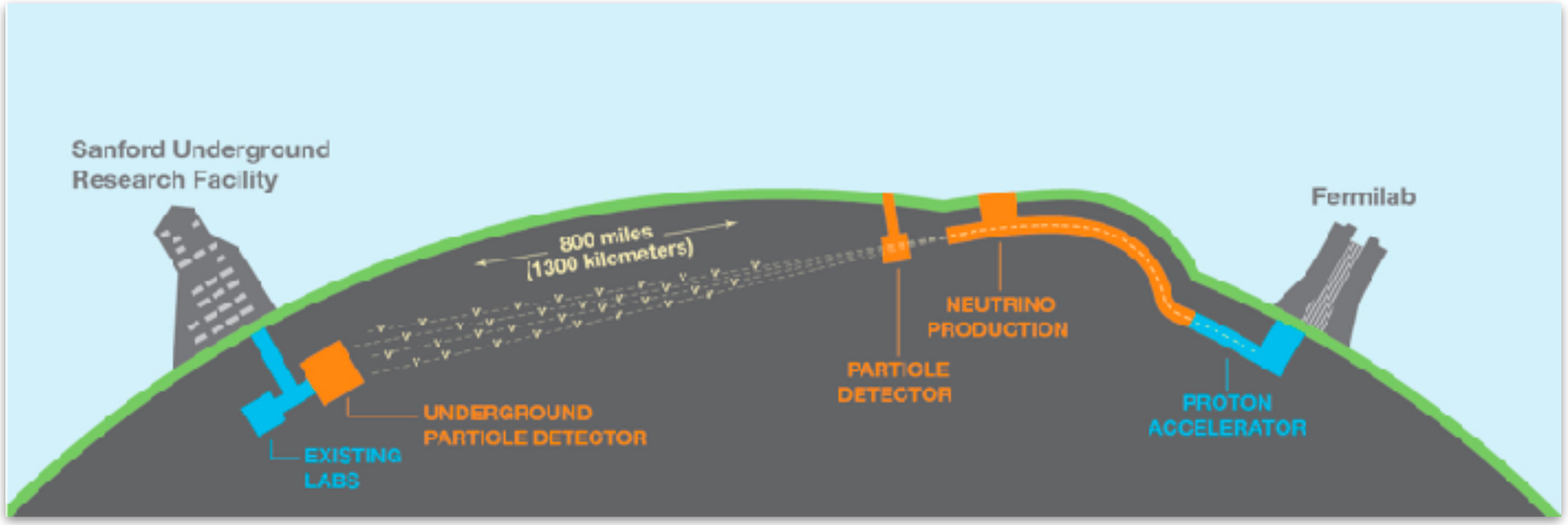

Neutrino experiments

Neutrino-oscillation and 0νββ experiments are (also) sensitive to the high-momentum components of the nuclear wave function

- Charge-parity (CP) violating phase and the mass hierarchy will be measured

- Determine whether the neutrino is a Majorana or a Dirac particle

- Need for including nuclear dynamics; mean-field models inadequate to describe neutrino-nucleus interaction

- A large body of experimental data for the electromagnetic cross sections of ^{4}He and ^{12}C (and many other nuclei) is available.

- A model unable to describe electron-nucleus scattering is (very) unlikely to describe neutrino-nucleus scattering.

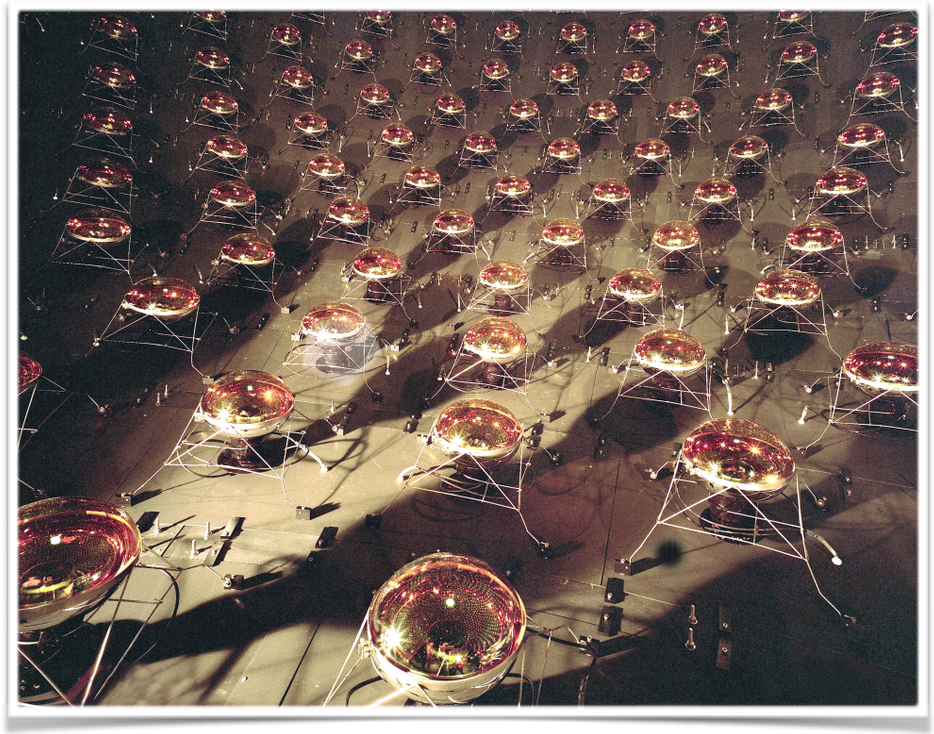

Lepton-nucleus scattering

Schematic representation of the inclusive cross section as a function of the energy loss.

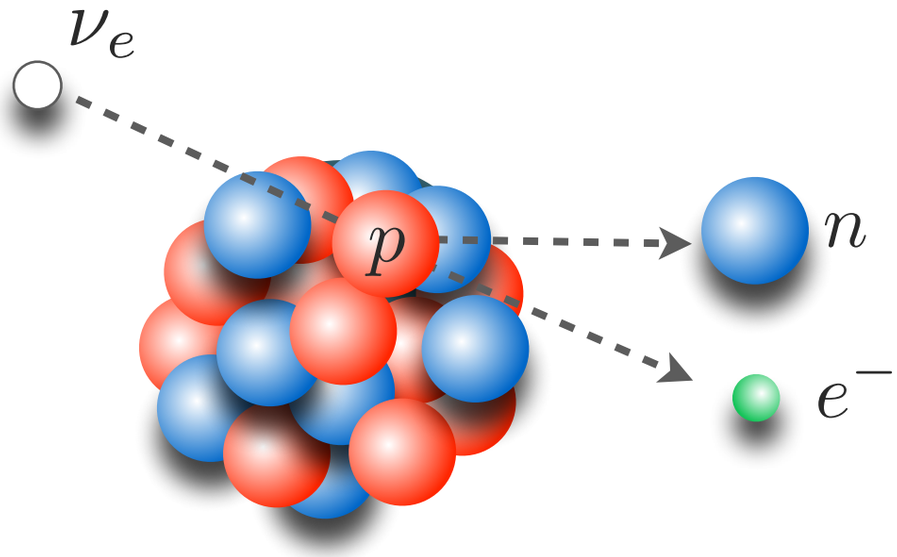

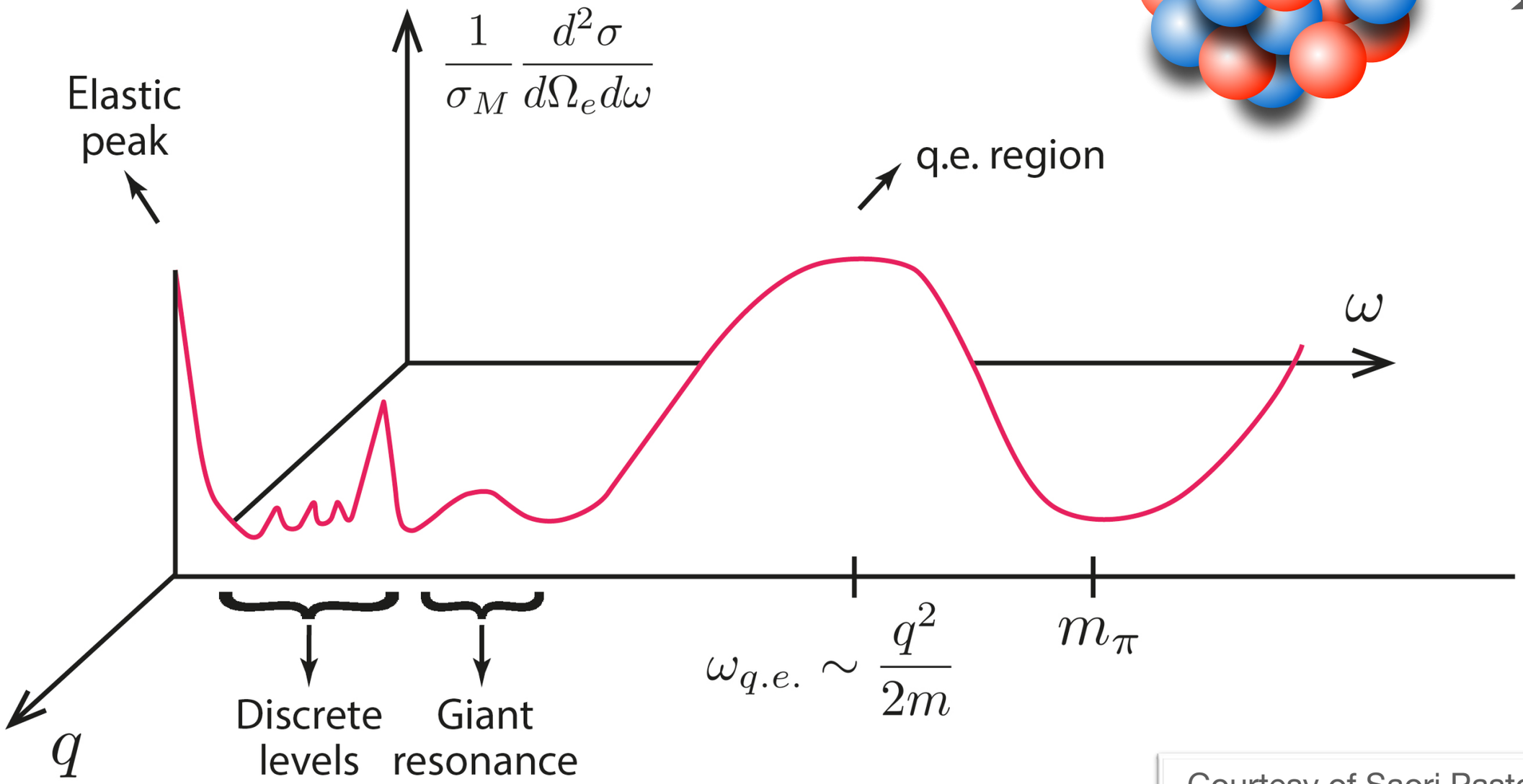

Courtesy of Saori Pastore

Lepton-nucleus scattering

The lepton-nucleus inclusive cross section is determined by **five response functions**

$$\frac{d\sigma}{dE_{\ell'}d\Omega_\ell} \propto [v_{00}R_{00} + v_{zz}R_{zz} - v_{0z}R_{0z} + v_{xx}R_{xx} \mp v_{xy}R_{xy}]$$

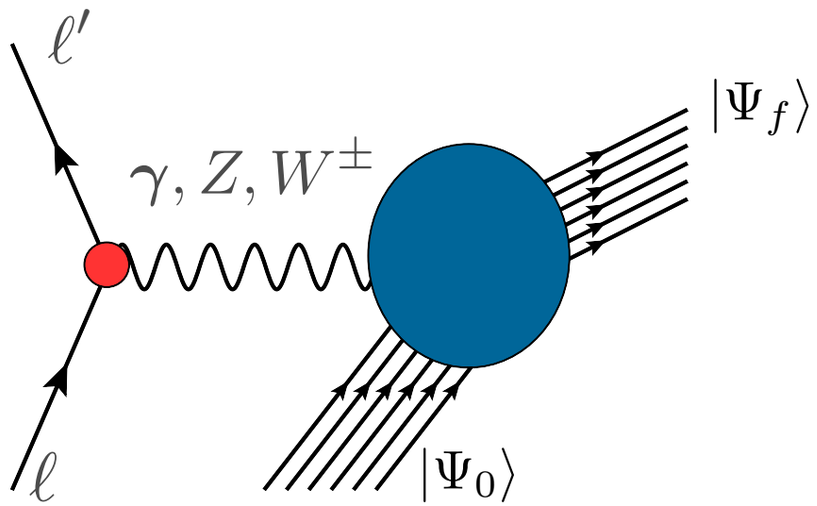

In electron scattering only the **longitudinal** and **transverse** responses contribute

The response functions contain all information on the structure and dynamics of the target

$$R_{\alpha\beta}(\omega, \mathbf{q}) = \sum_f \langle\Psi_0|J^\dagger_\alpha(\mathbf{q})|\Psi_f\rangle\langle\Psi_f|J_\beta(\mathbf{q})|\Psi_0\rangle\delta(\omega - E_f + E_0)$$

They include initial-state correlations, final state correlations and two-body currents

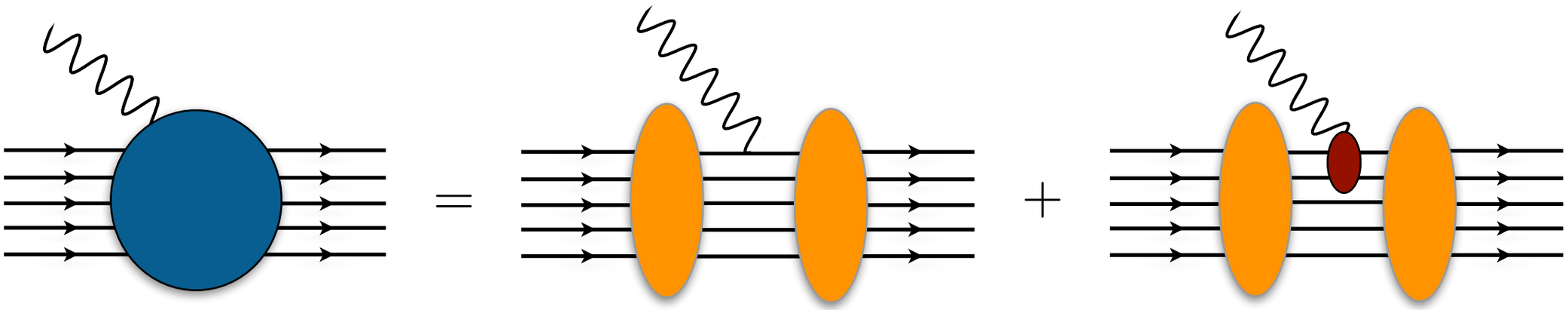

Moderate momentum-transfer regime

Up to moderate values of the momentum transfer, both initial and final states are eigenstates of the nuclear Hamiltonian

$$H|\Psi_0\rangle = E_0|\Psi_0\rangle \qquad H|\Psi_f\rangle = E_f|\Psi_f\rangle$$

As for the electron scattering on ^{12}C

$$|^{12}\mathrm{C}^*\rangle,\ |^{11}\mathrm{B}, p\rangle,\ |^{11}\mathrm{C}, n\rangle,\ |^{10}\mathrm{B}, pn\rangle,\ |^{9}\mathrm{Be}, pp\rangle,\ |^{9}\mathrm{C}, nn\rangle \ldots$$

The **integral transform** of the response function are defined as

$$E_{\alpha\beta}(\sigma, \mathbf{q}) \equiv \int d\omega K(\sigma, \omega) R_{\alpha\beta}(\omega, \mathbf{q})$$

$$R_{\alpha\beta}(\omega, \mathbf{q}) = \sum_f \langle\Psi_0|J^\dagger_\alpha(\mathbf{q})|\Psi_f\rangle\langle\Psi_f|J_\beta(\mathbf{q})|\Psi_0\rangle\delta(\omega - E_f + E_0)$$

Using the completeness of the final states, the integral transform is expressed as **ground-state expectation values**

$$E_{\alpha\beta}(\sigma, \mathbf{q}) = \langle\Psi_0|J^\dagger_\alpha(\mathbf{q})K(\sigma, H - E_0)J_\beta(\mathbf{q})|\Psi_0\rangle$$

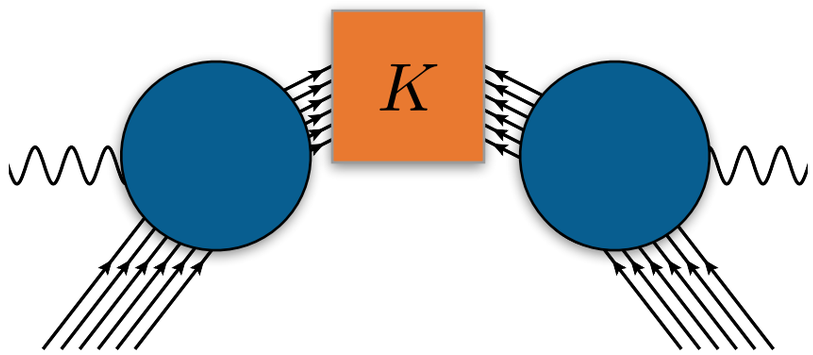

Lorentz integral transform (LIT)

- The Lorentz integral transform

$$K(\sigma,\omega) = \frac{1}{(\omega-\sigma_R)^2+\sigma_I^2}$$

has been successfully exploited in the calculation of electromagnetic and neutral-weak responses

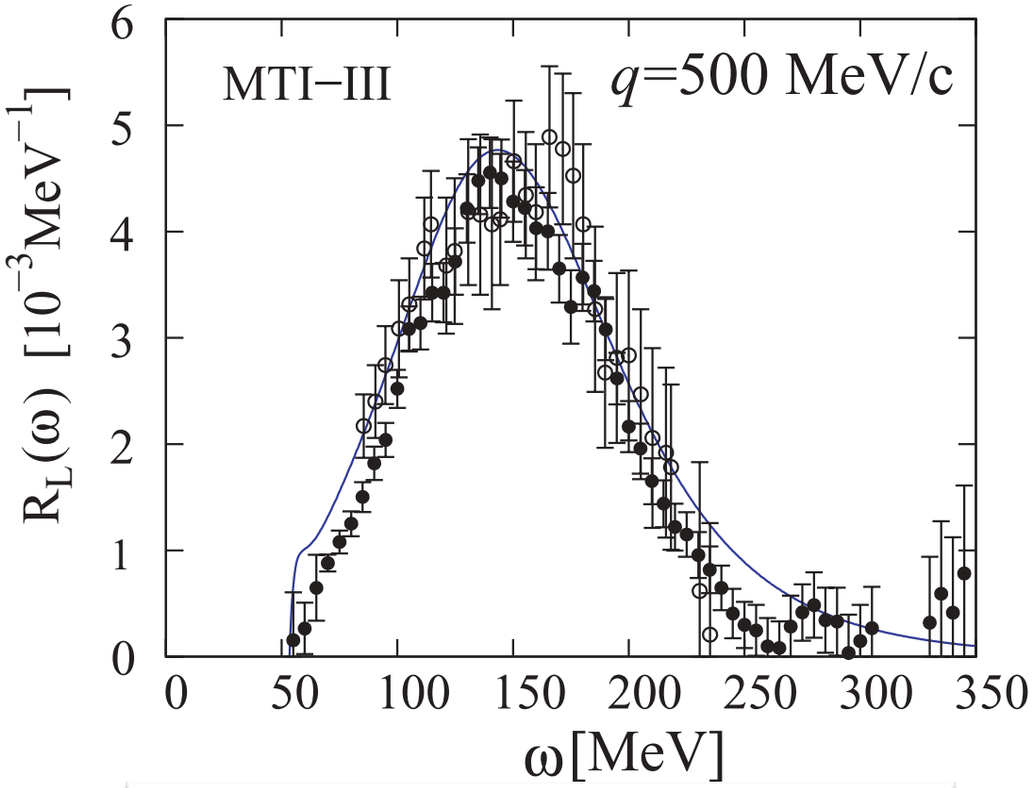

S. Bacca et al., PRC **76**, 014003 (2007)

S. Bacca et al., PRL **111**, 122502 (2013)

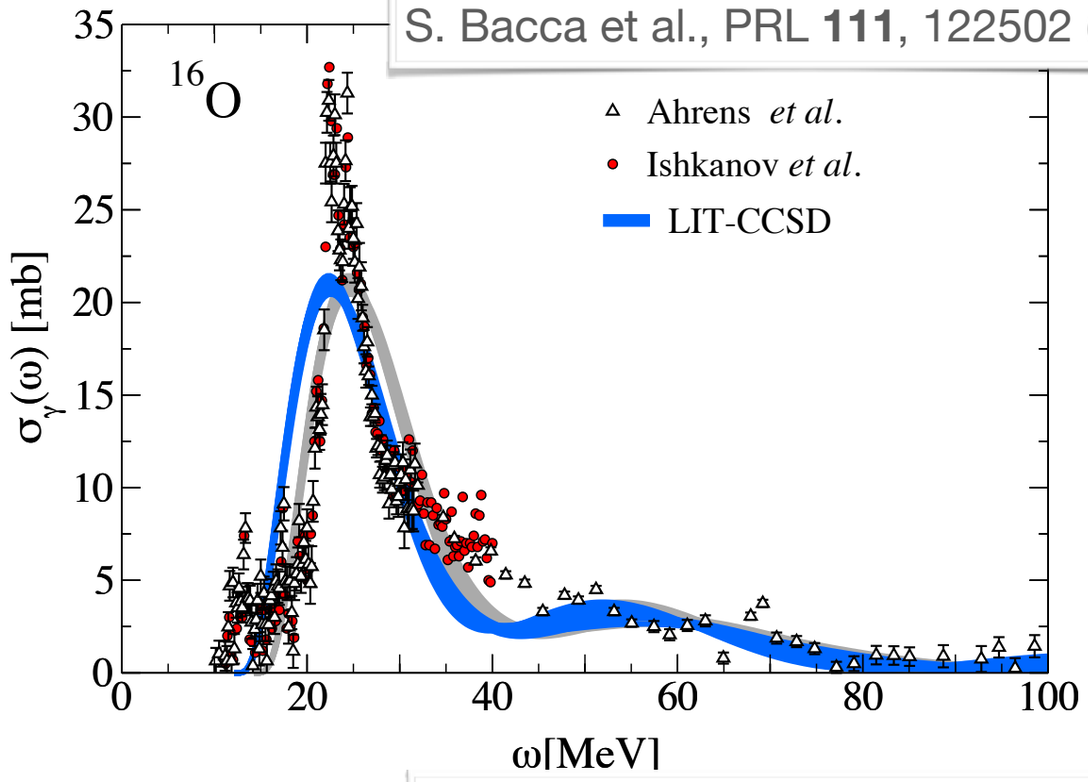

S. Bacca et al., PRC **6**, 064619 (2014)

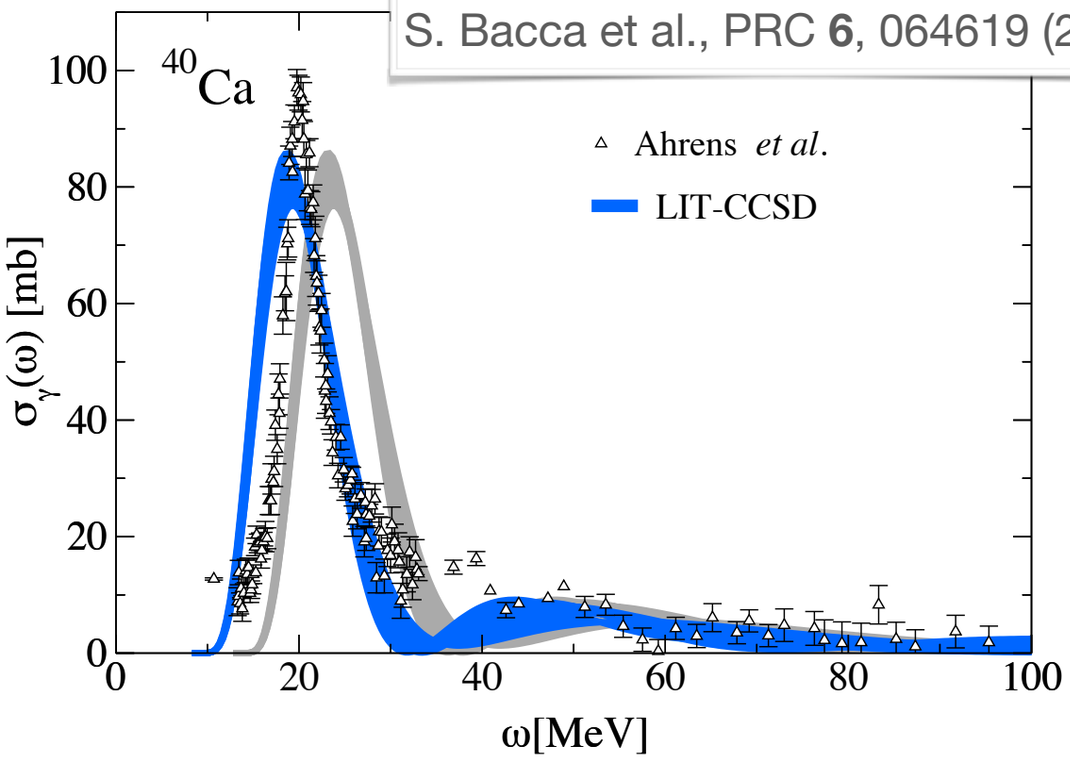

Euclidean response function

Valuable information on the energy dependence of the response functions can be inferred from their **Laplace transforms**

$$E_{\alpha\beta}(\tau, \mathbf{q}) \equiv \int d\omega e^{-\omega\tau} R_{\alpha\beta}(\omega, \mathbf{q})$$

At finite imaginary time the contributions from large energy transfer are quickly suppressed

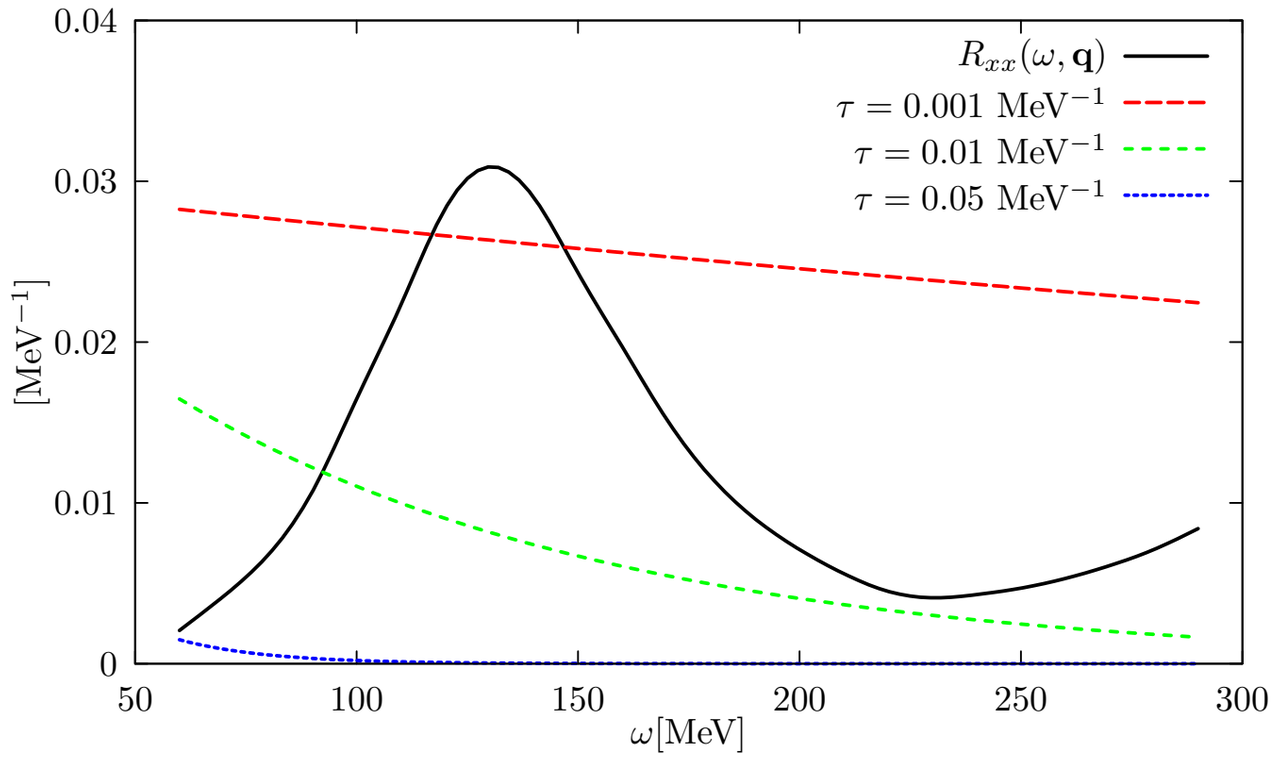

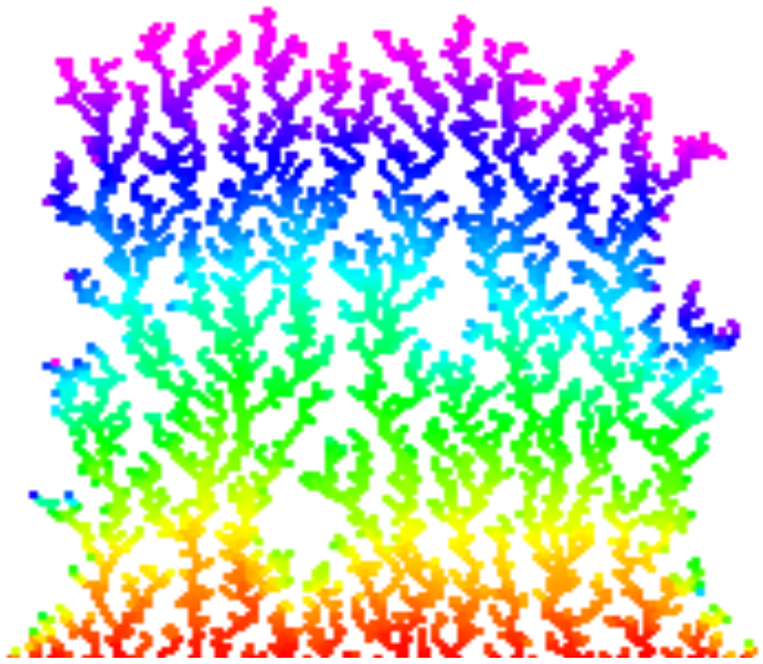

The system is first heated up by the transition operator.
Its cooling determines the **Euclidean response** of the system

$$\sum_f |\Psi_f\rangle\langle\Psi_f|$$

$$E_{\alpha\beta}(\tau, \mathbf{q}) = \langle\Psi_0|J^\dagger_\alpha(\mathbf{q}) e^{-(H-E_0)\tau} J_\beta(\mathbf{q})|\Psi_0\rangle$$

Analogous techniques are used in Lattice QCD and condensed matter Physics

(Future) Inversion of the Euclidean response

The Euclidean response formalism allows one to extract dynamical properties of the system from ground-state calculations

Inverting the Euclidean response is an ill posed problem: any set of observations is limited and noisy and the situation is even worse since the kernel is a smoothing operator.

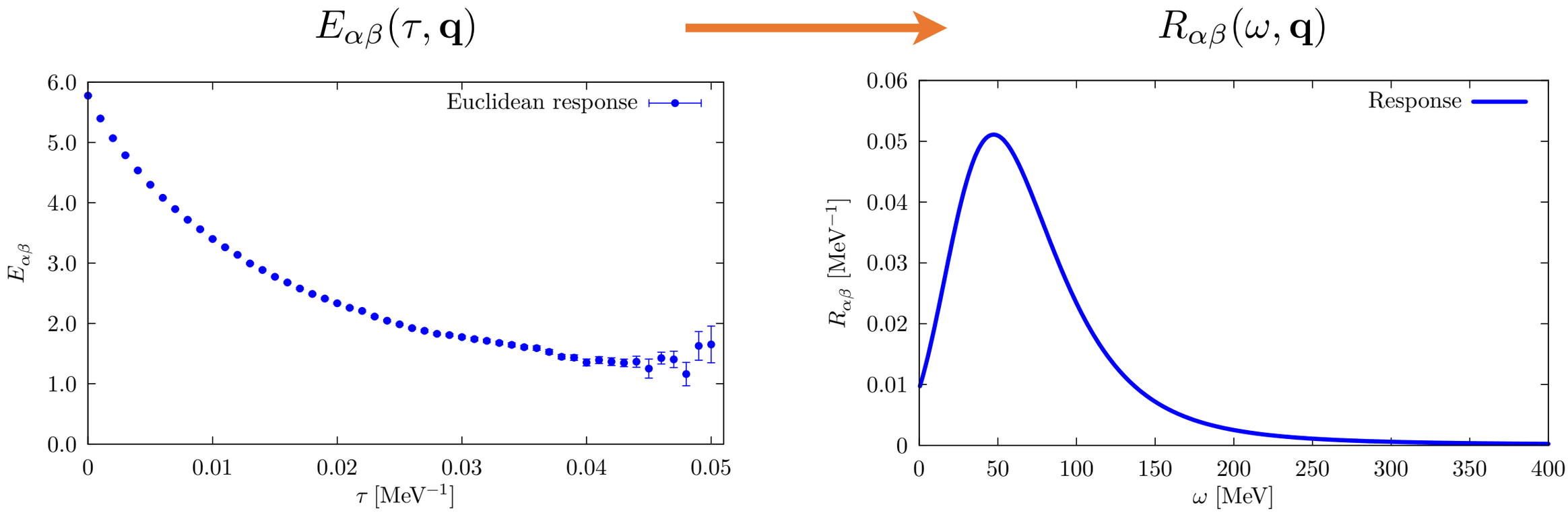

Maximum-entropy techniques are reliable enough for quasi-elastic responses

We are now exploring new strategies, based on **deep learning techniques**, to improve the accuracy of the inversion and to better estimate the associated uncertainties

^{12}C electromagnetic response

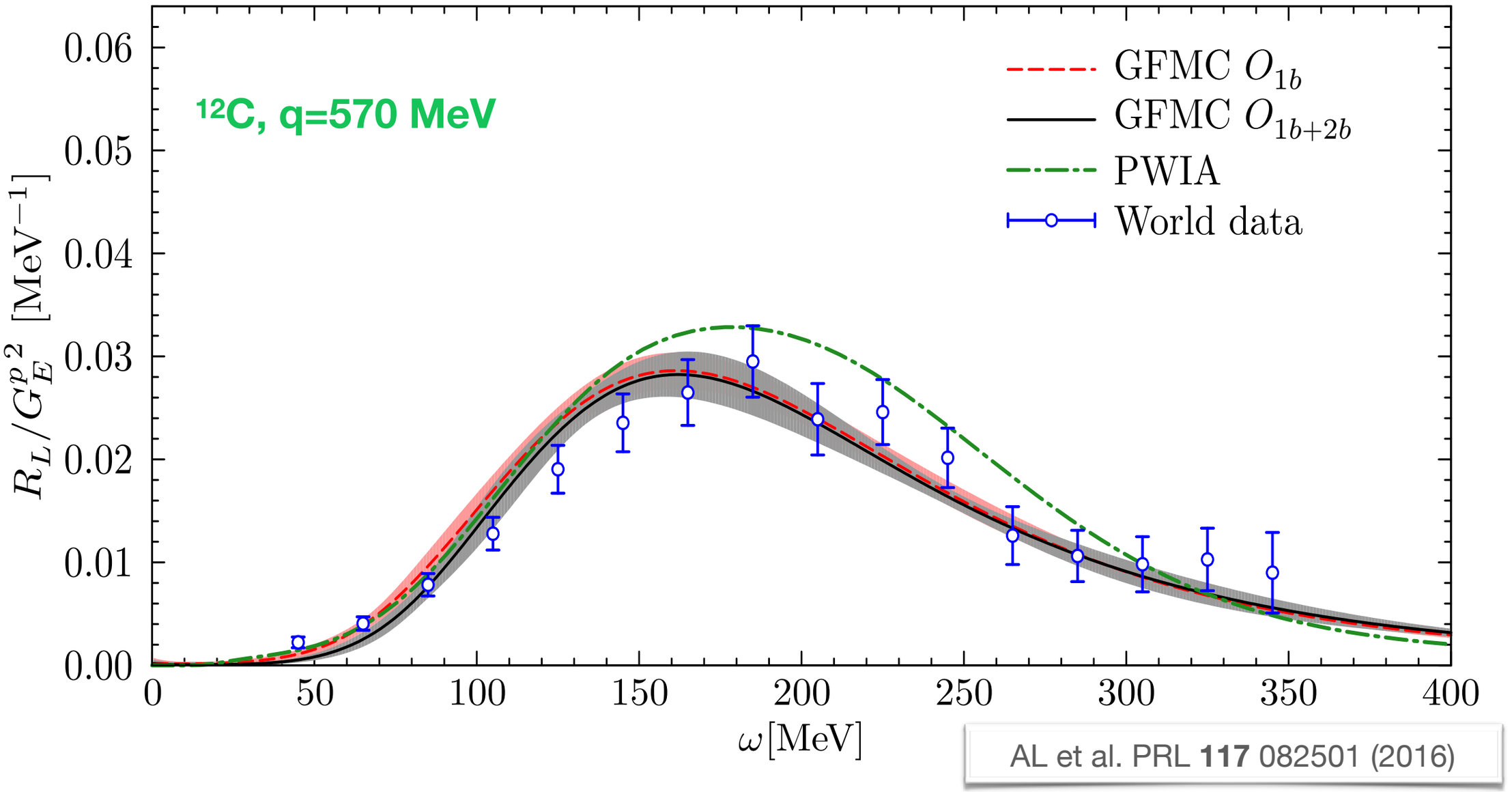

AL et al. PRL **117** 082501 (2016)

- Correlations and interaction effects in the final states redistribute strength from the quasi-elastic peak to high-energy transfer regions
- Good agreement with data **without in-medium modifications** of the nucleon form factors
- Small contribution from two-body currents.

^{12}C electromagnetic response

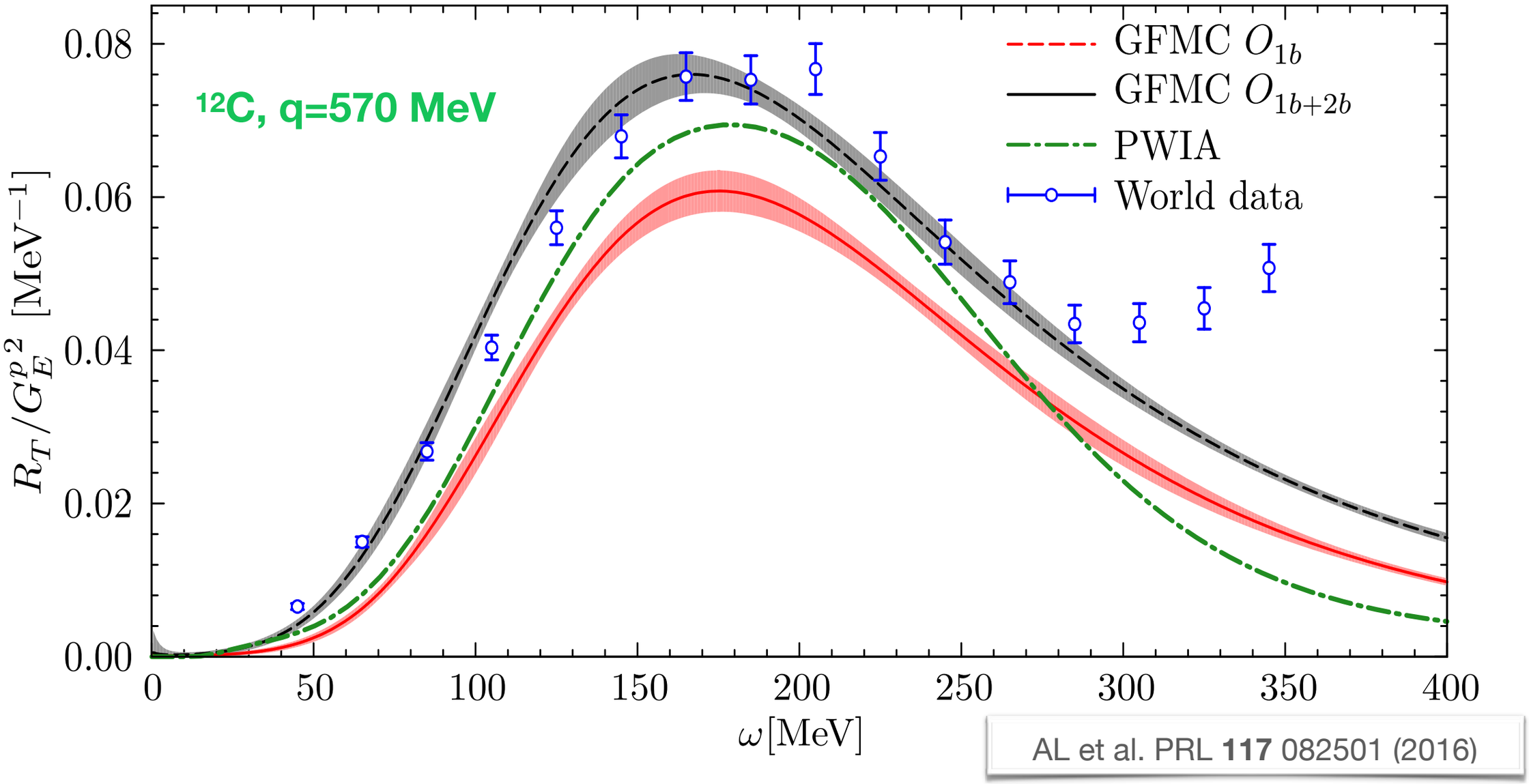

AL et al. PRL **117** 082501 (2016)

- Two-body currents generate a **large excess of strength** in over the whole quasi-elastic region
- Correlations and interaction effects in the final states redistribute strength from the quasi-elastic peak to high-energy transfer regions
- Need to include relativistic corrections in the kinematics

^{12}C neutral-current cross-section

- The anti-neutrino cross section decreases rapidly relative to the neutrino cross section as the scattering angle changes from the forward to the backward hemisphere
- **Sizable enhancement from two-body currents**, more effective for neutrino than for anti-neutrino

$$\sigma \propto [v_{00}R_{00} + v_{zz}R_{zz} - v_{0z}R_{0z} + v_{xx}R_{xx} \mp v_{xy}R_{xy}]$$

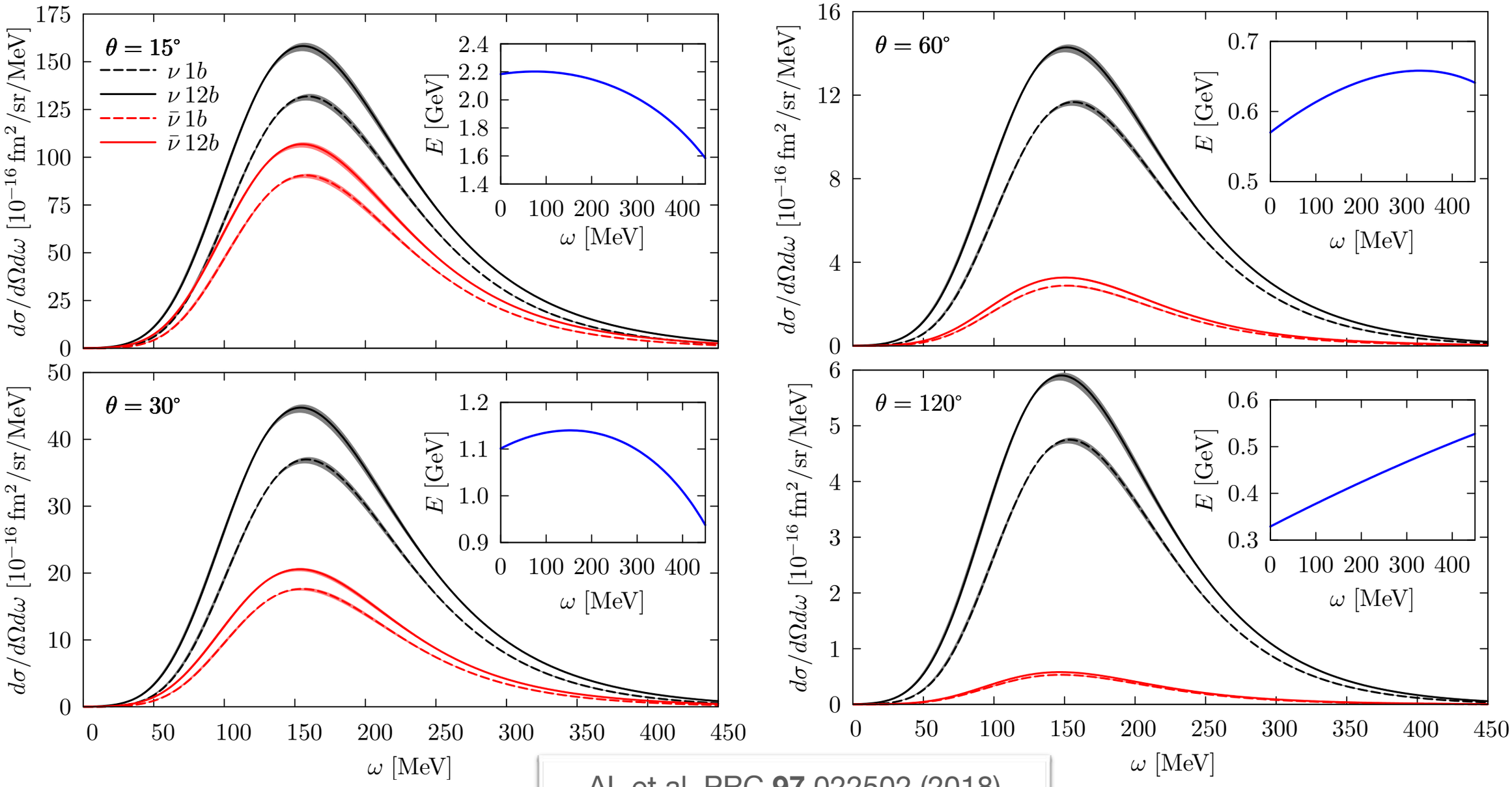

AL et al. PRC **97** 022502 (2018)

^{12}C charged-current responses

Computing charged-current reactions required **extending the GFMC** to propagate intermediate states with different numbers of protons and neutrons compared to the ground state

Two-body currents have **little effect in the vector term**, but enhance the axial contribution at energy larger than quasi-elastic kinematics

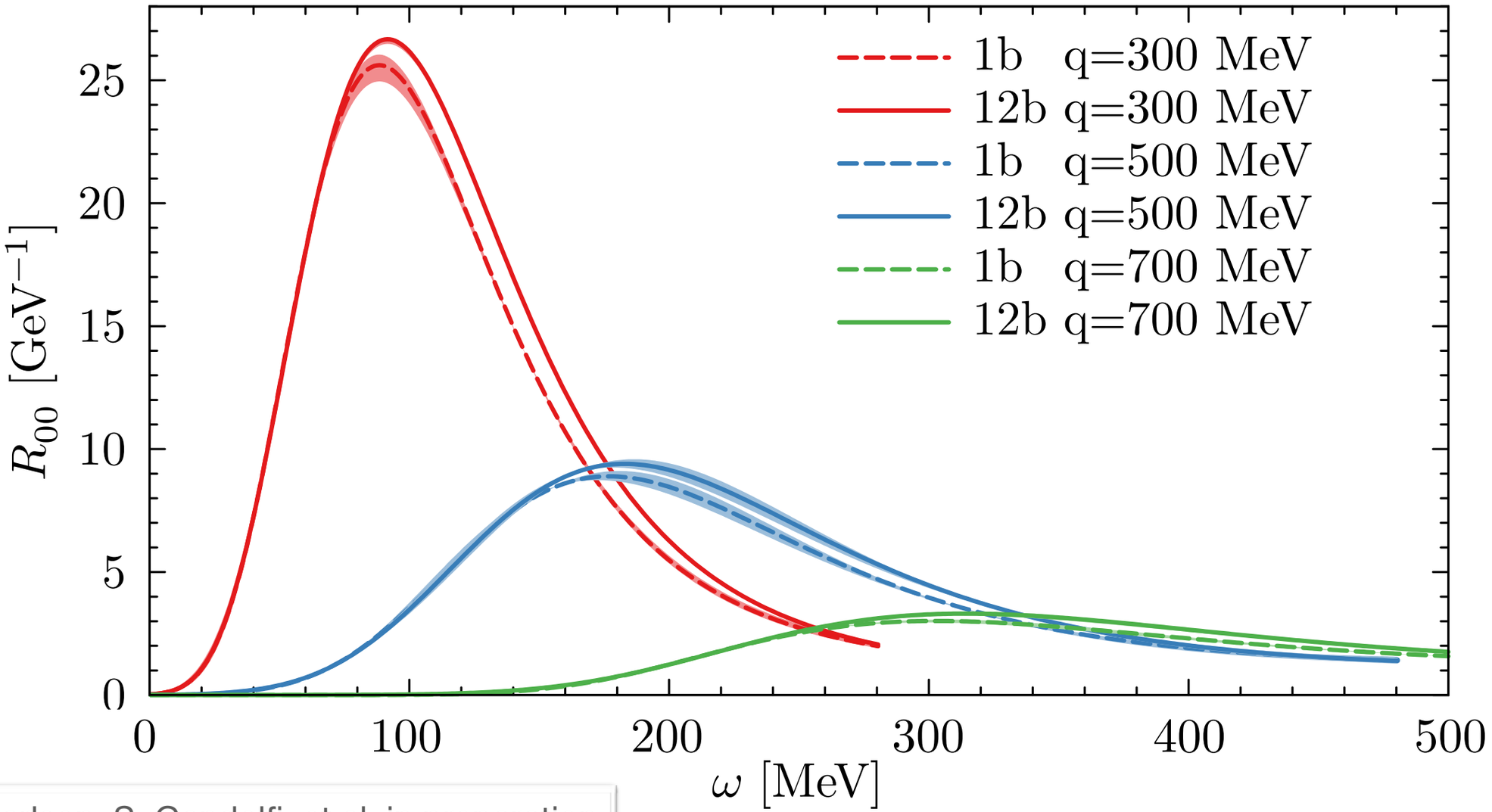

AL, J. Carlson, S. Gandolfi, et al. in preparation

^{12}C charged-current responses

Computing charged-current reactions required **extending the GFMC** to propagate intermediate states with different numbers of protons and neutrons compared to the ground state

Two-body currents have a **sizable effect in the transverse response,** both in the vector and in the axial contributions

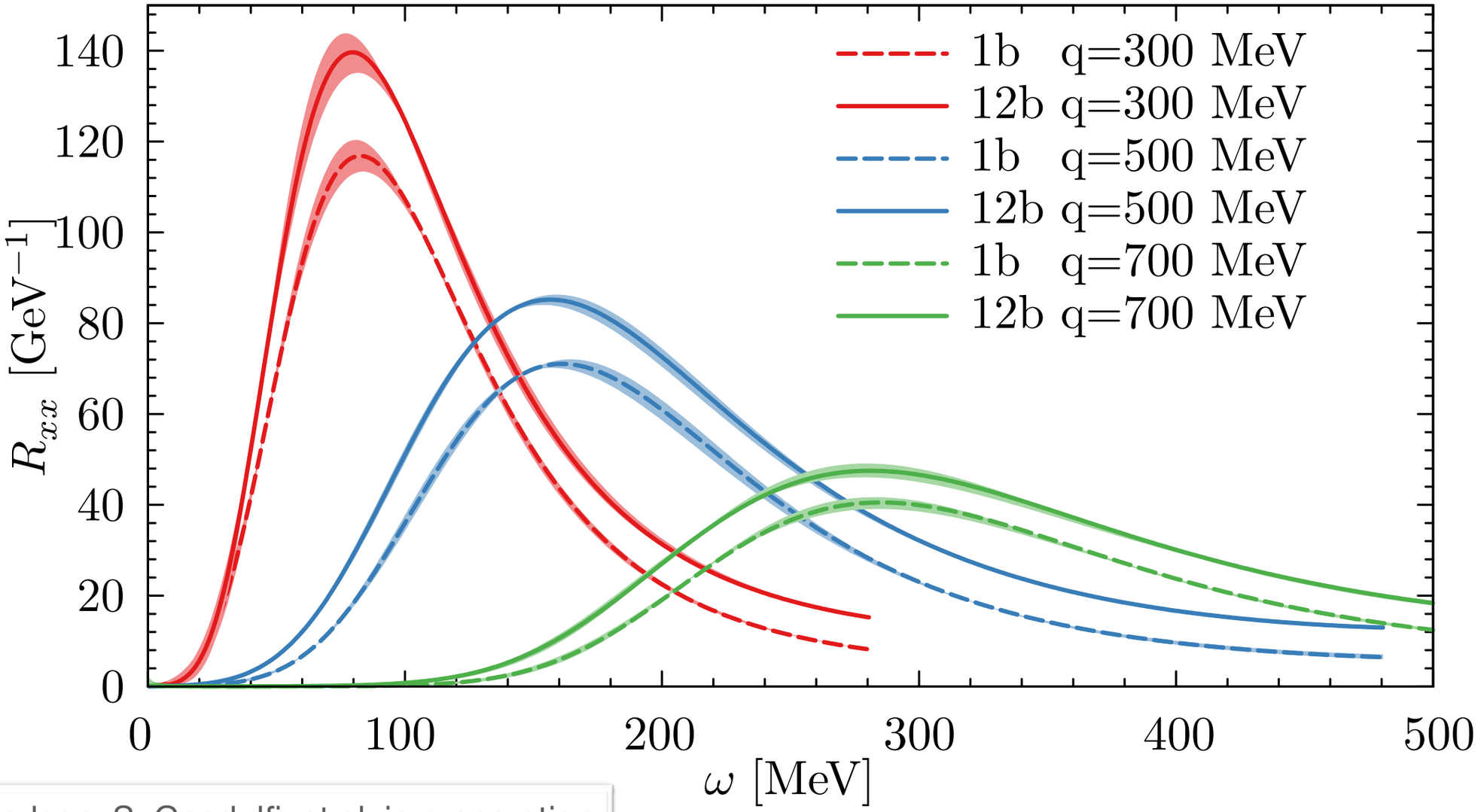

AL, J. Carlson, S. Gandolfi, et al. in preparation

^{12}C charged-current responses

Computing charged-current reactions required **extending the GFMC** to propagate intermediate states with different numbers of protons and neutrons compared to the ground state

Two-body currents have a **sizable effect in the interference between the axial and vector current contributions**, important to asses neutrino/antineutrino event rates

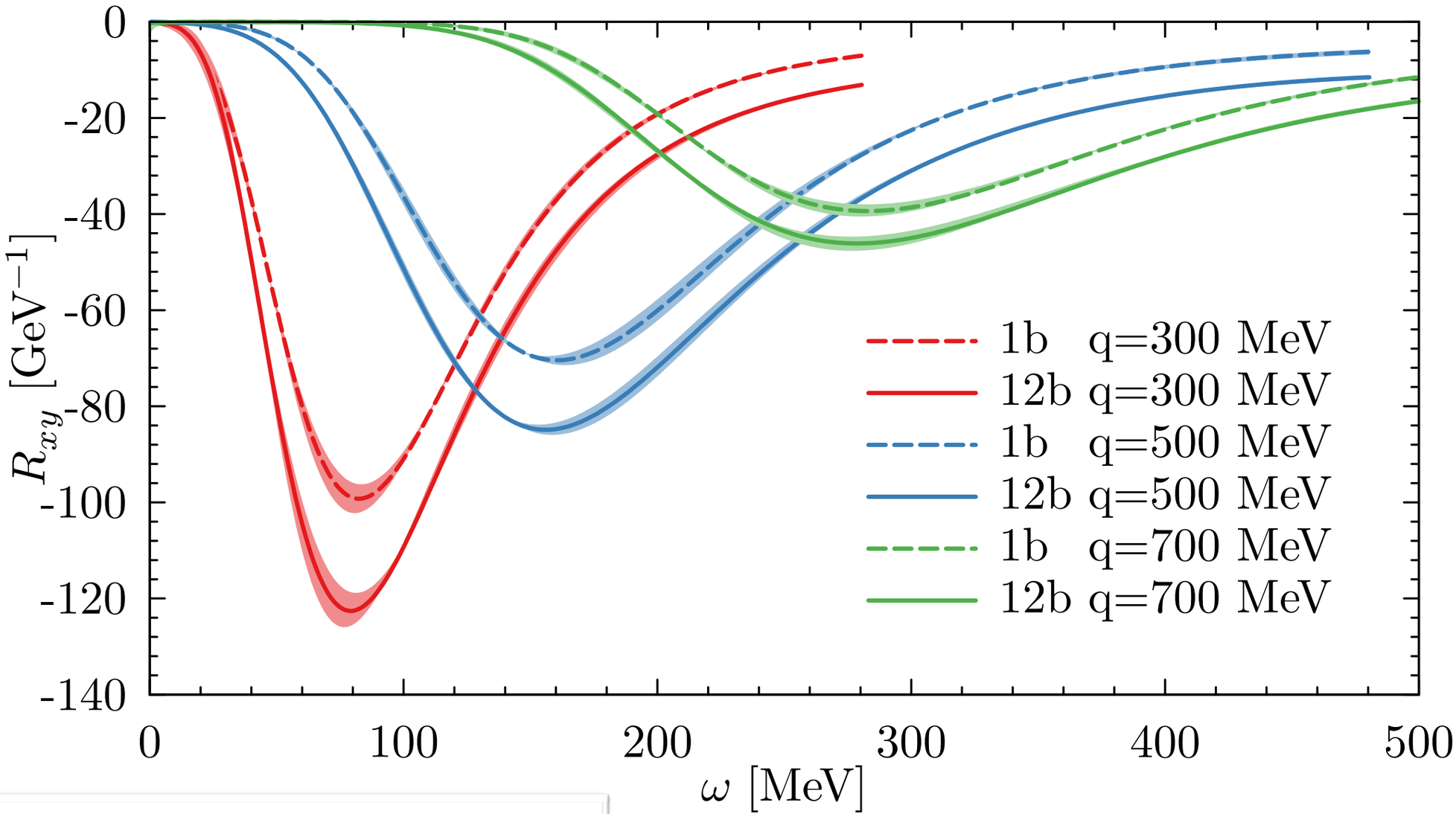

AL, J. Carlson, S. Gandolfi, et al. in preparation

^{12}C charged-current cross sections

To obtain the inclusive cross section, we interpolate the response functions and fold the cross section with the fluxes of the MiniBooNE and T2K experiments

$$\left\langle \frac{d\sigma}{dT_\mu \, d\cos\theta_\mu} \right\rangle = \int dE_\nu \, \phi(E_\nu) \, \frac{d\sigma(E_\nu)}{dT_\mu \, d\cos\theta_\mu} \ ,$$

The energy of neutrino beams, produced as secondary decay products, is not monochromatic

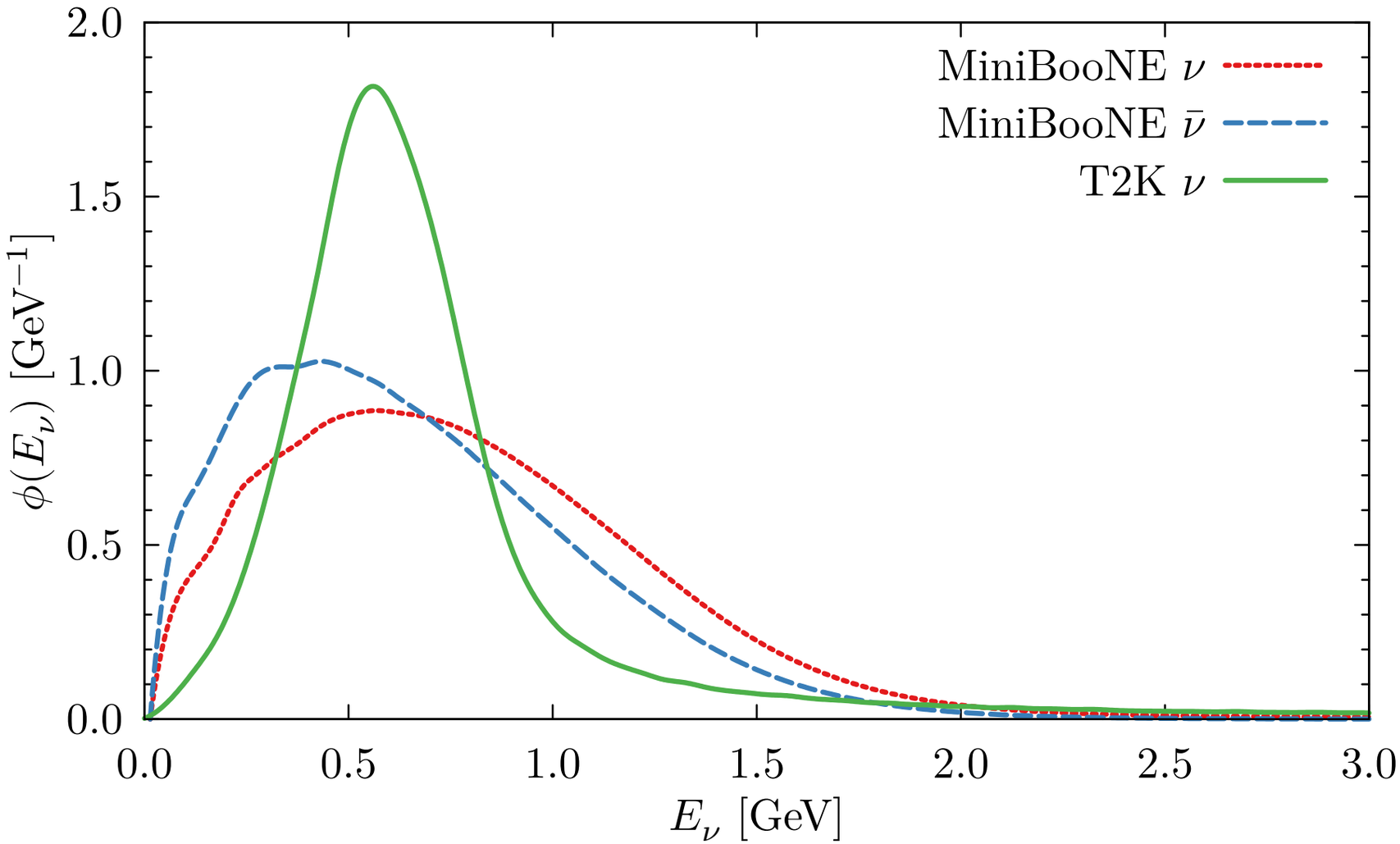

MiniBoone cross sections

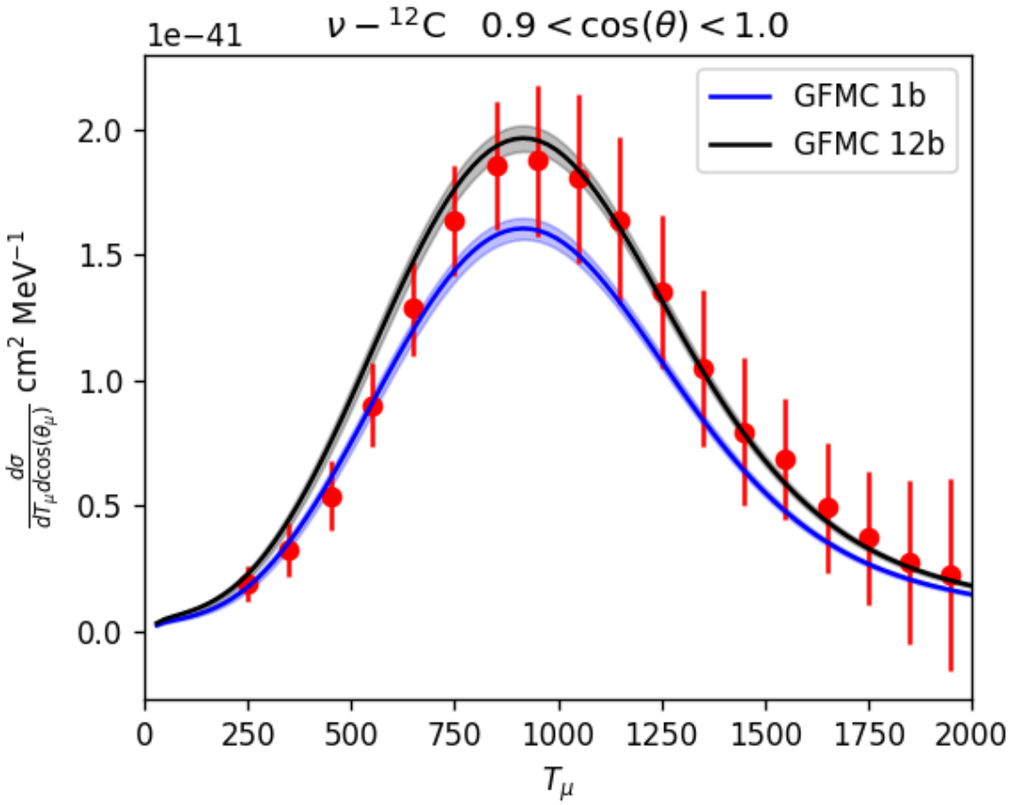

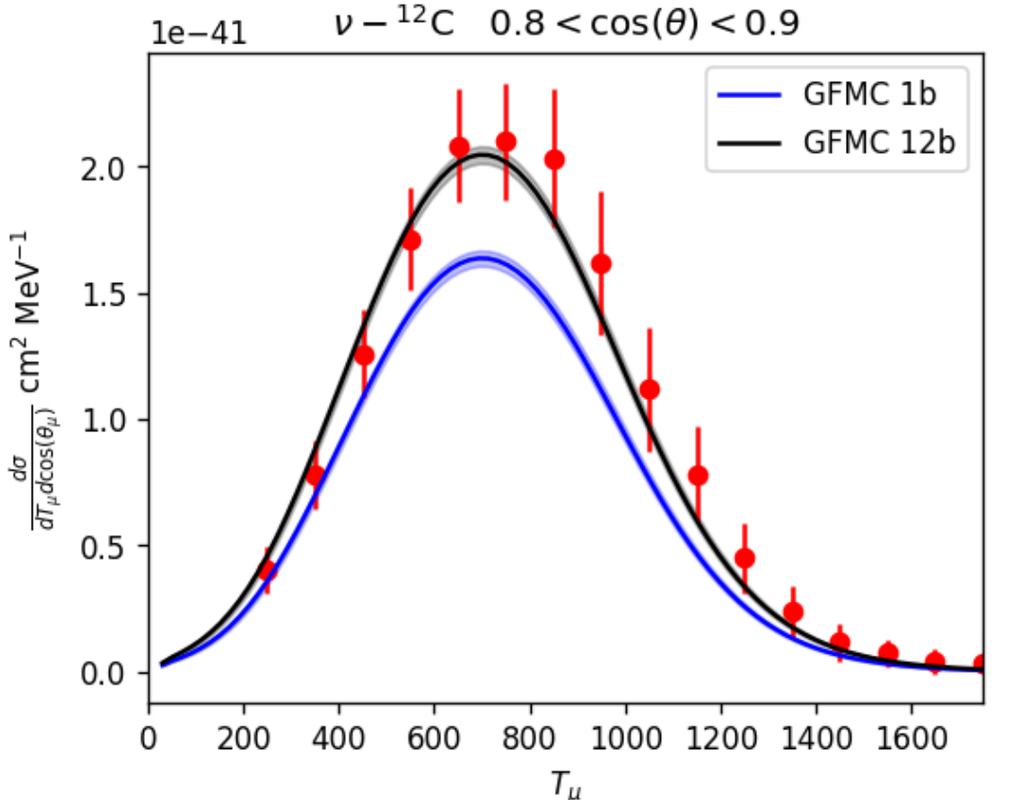

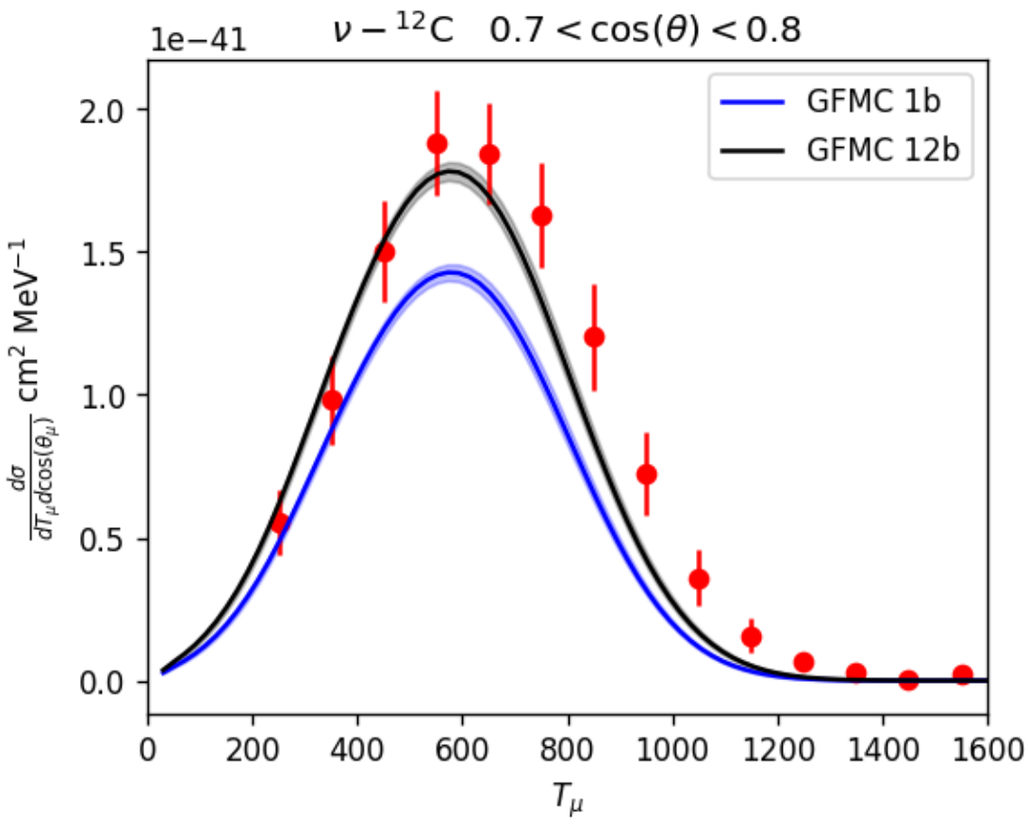

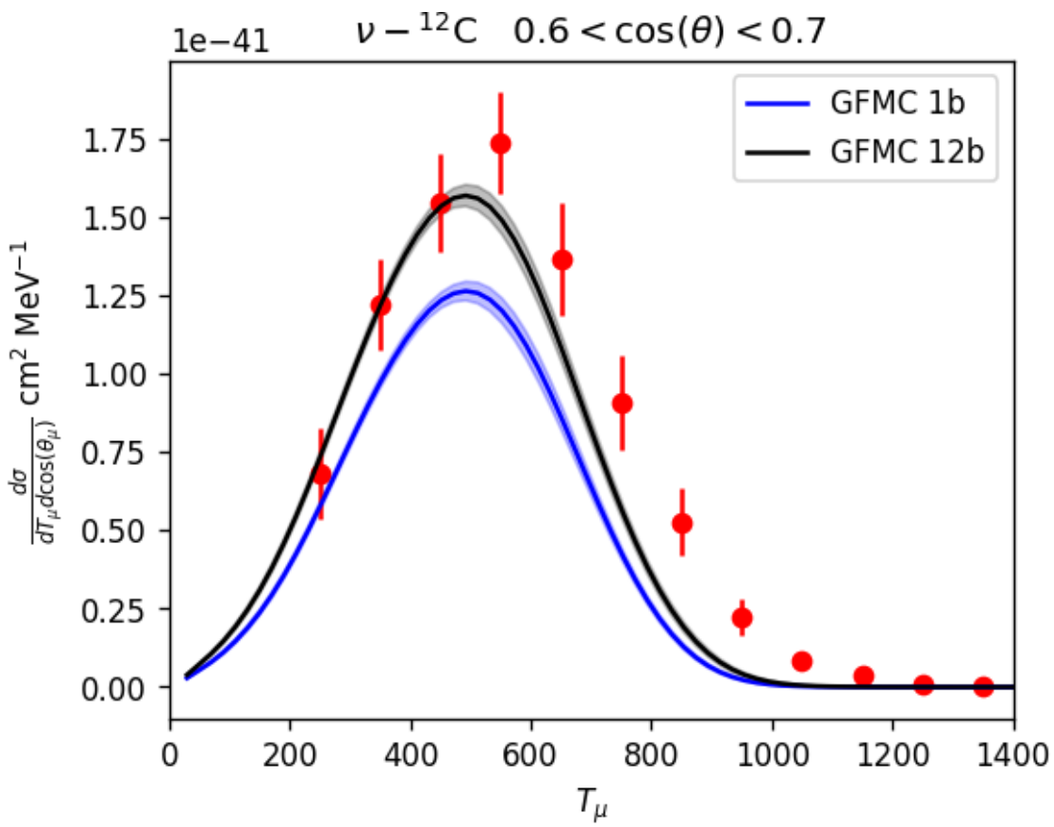

MiniBoone cross sections

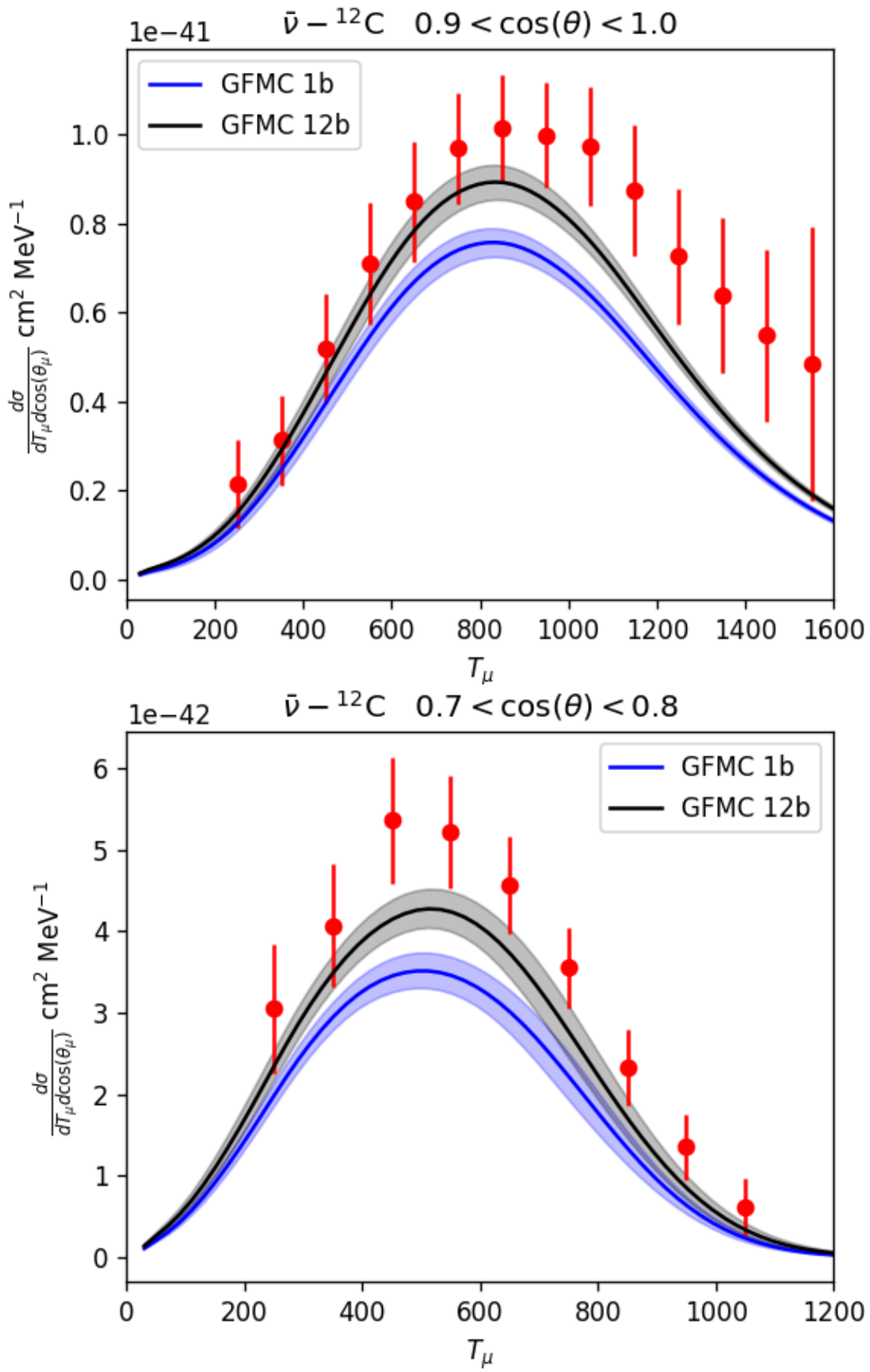

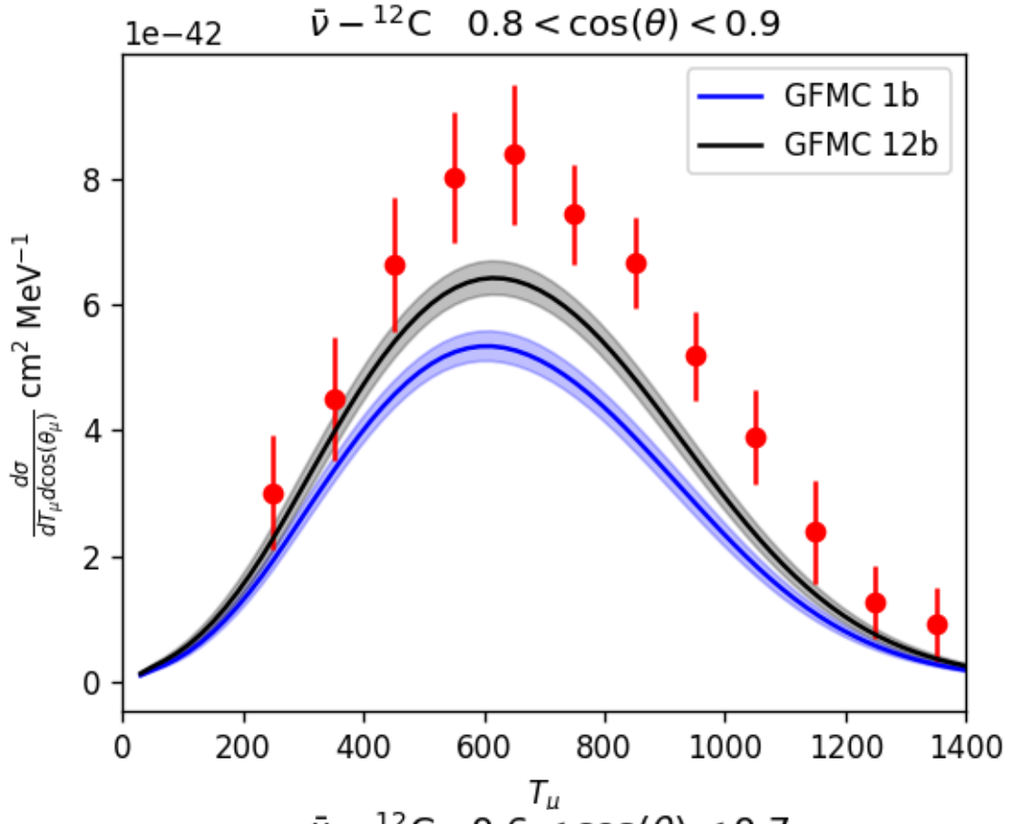

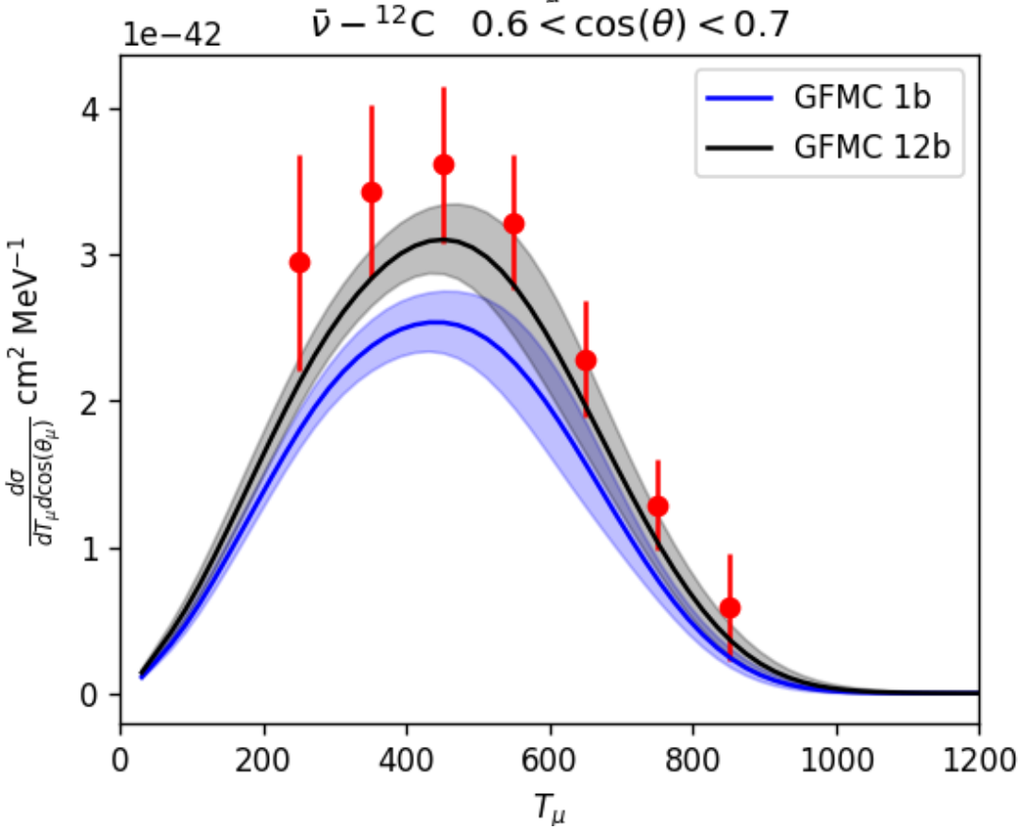

T2K cross sections

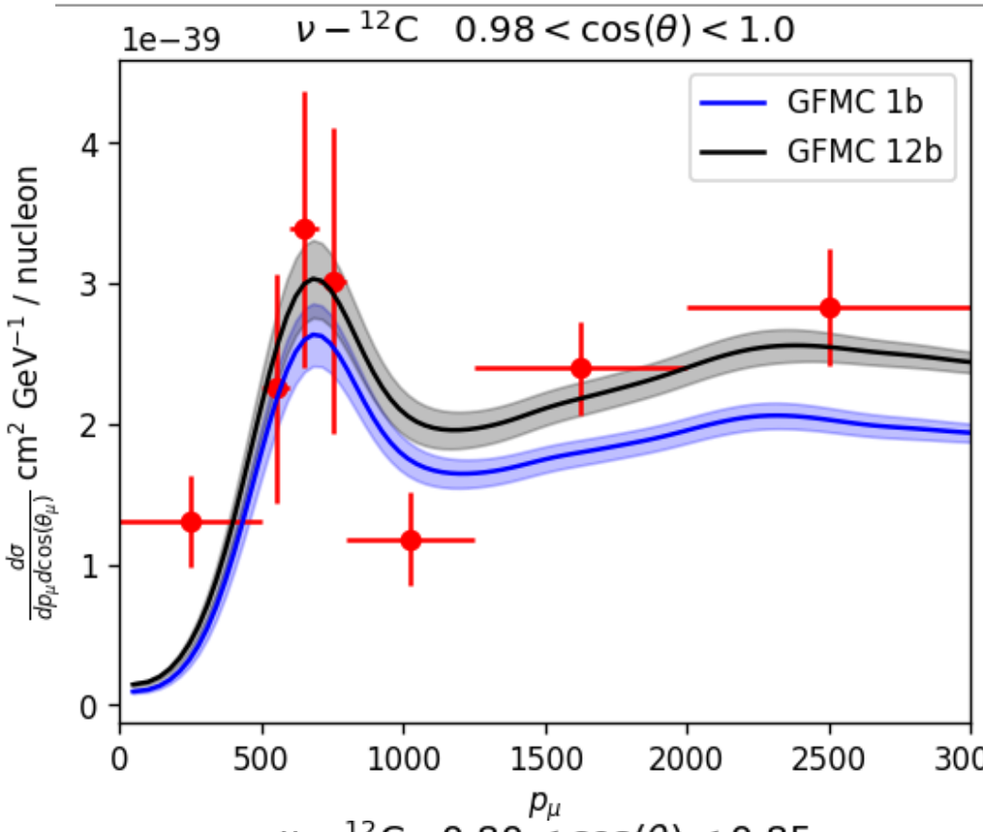

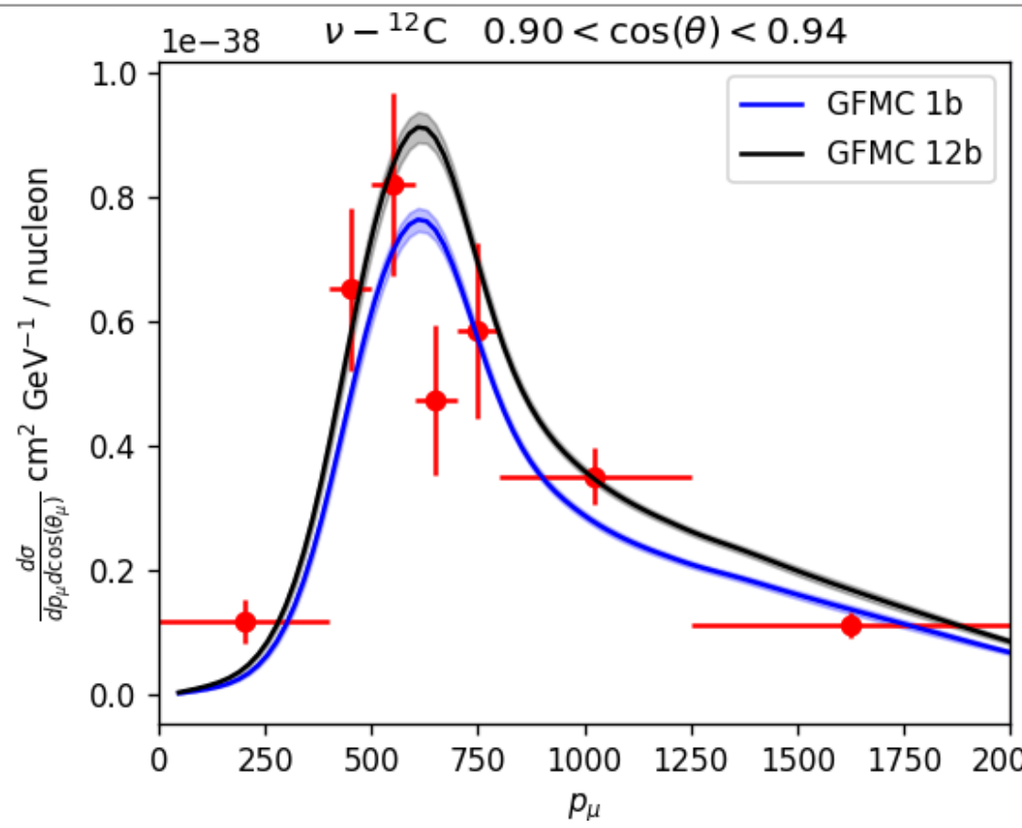

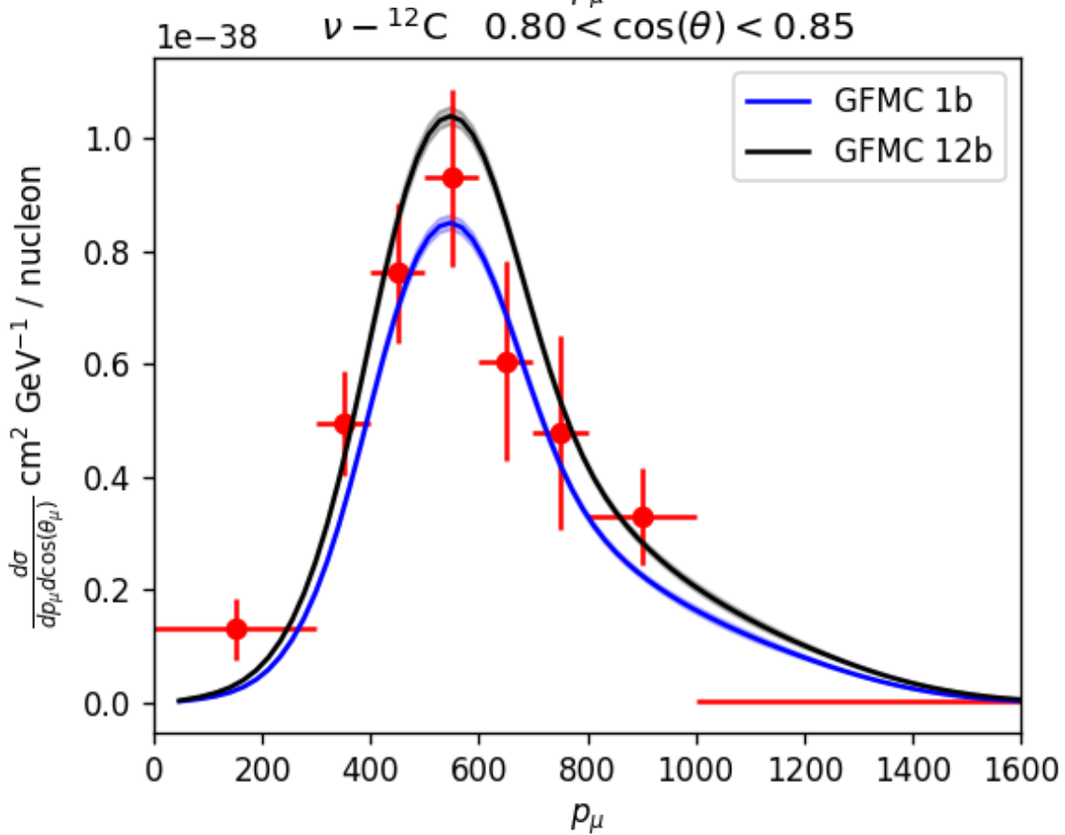

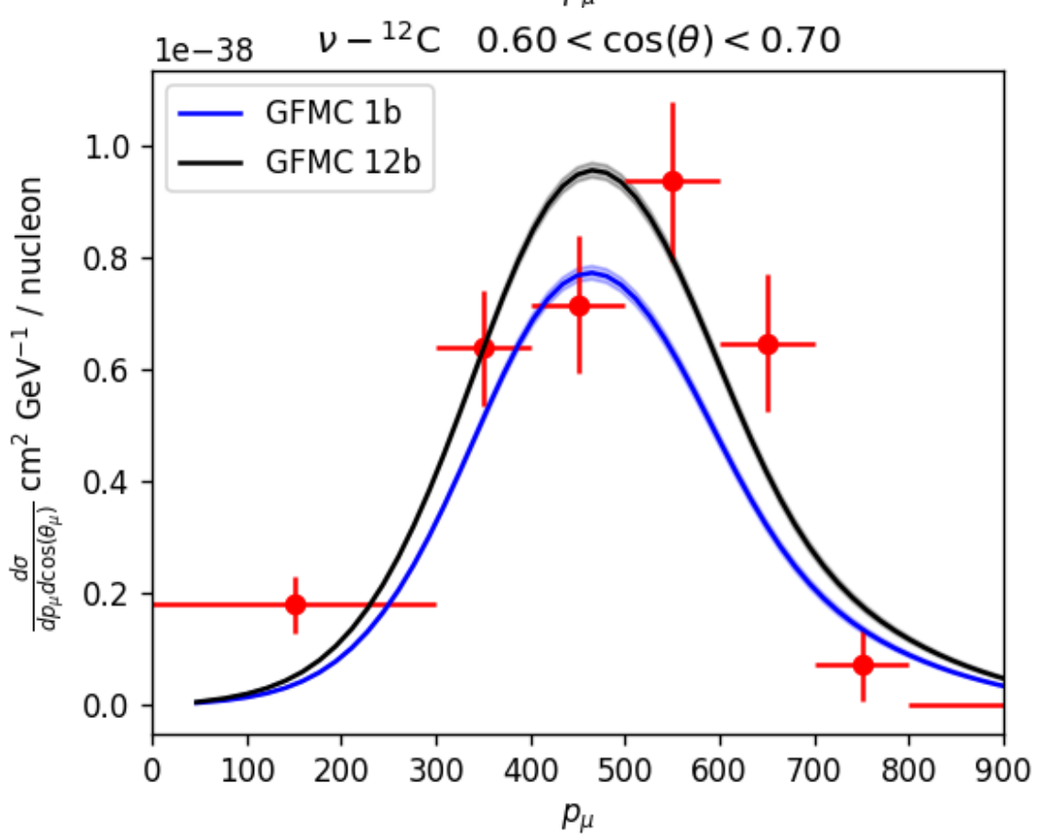

Momentum scales in neutrino interactions

Oscillation experiments

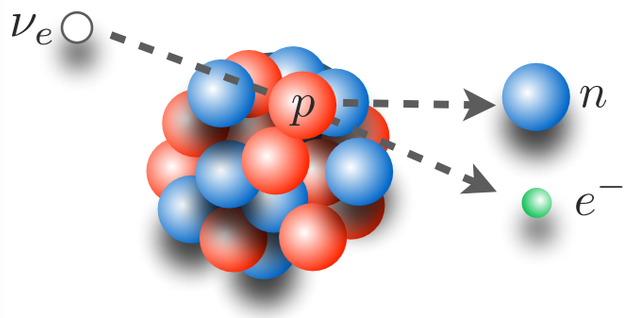

0νββ decays

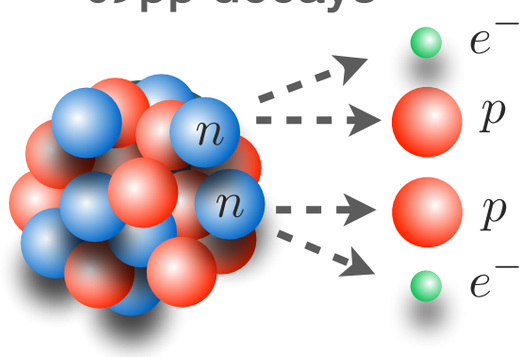

Single-beta decays

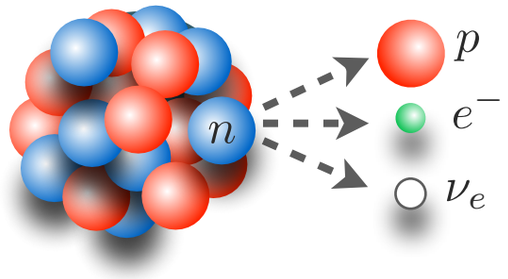

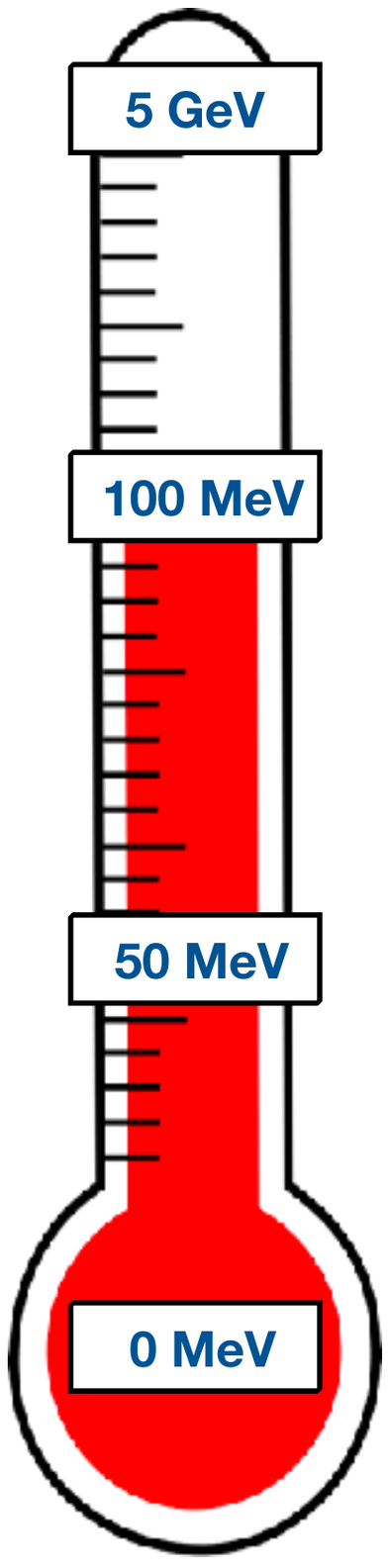

Muon capture

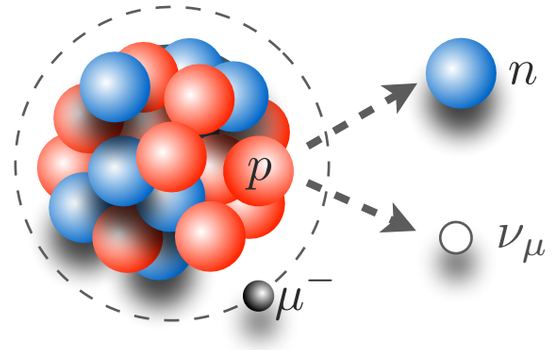

Neutron-star cooling

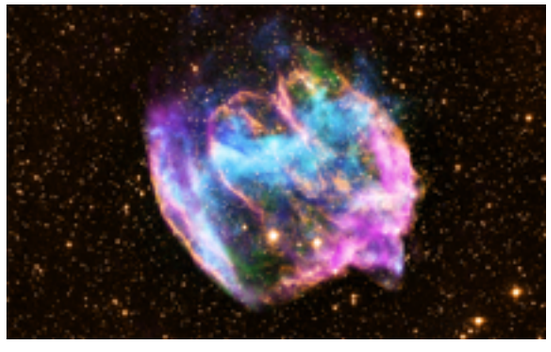

Muon capture in ^{3}H and ^{4}He

To **validate our model of nuclear dynamics** at intermediate values of momentum transfer we computed the total muon-capture rate of 4He

- Role of **two-body axial terms**
- Single-nucleon **axial form factor**

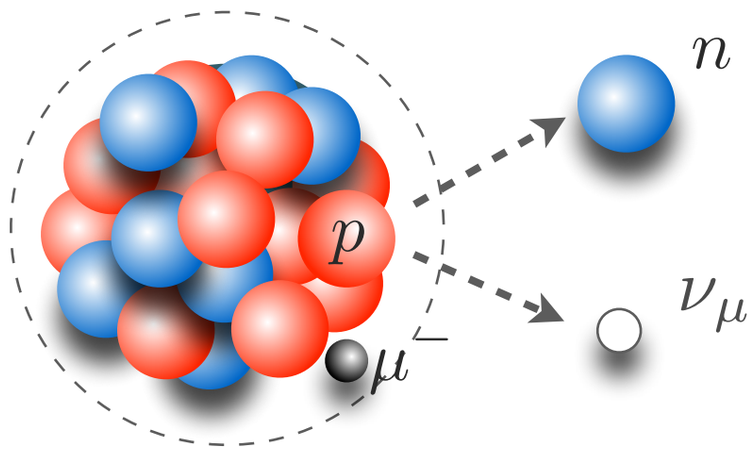

AL, et al. PRC **100,** 035502 (2019)

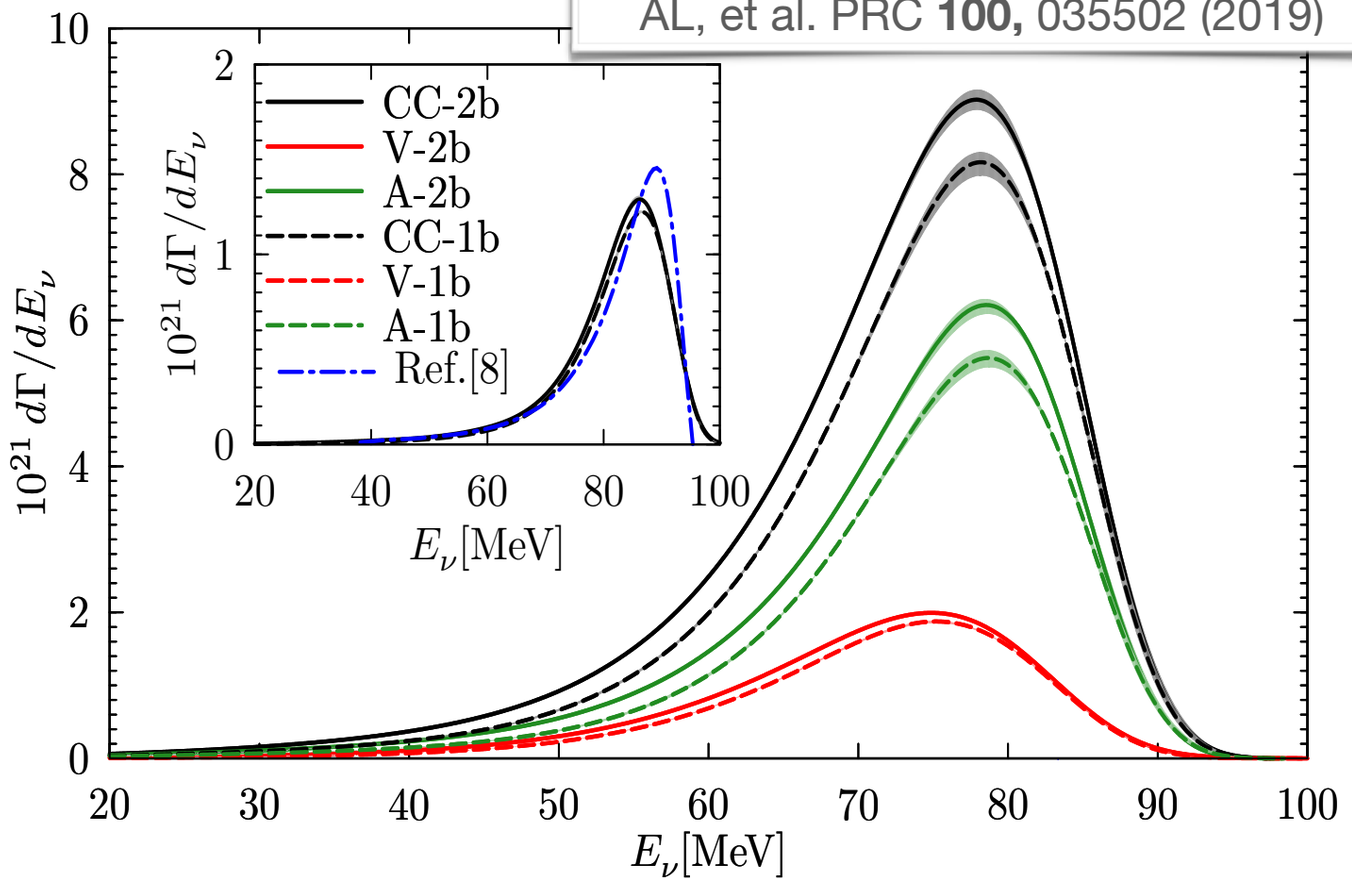

Excellent agreement with available data, which have large errors. **New measurements?**

	CC-1b	CC-2b	Exp [54]	Exp [55]	Exp [56]	Th [57]	Th [58]
$\Gamma(\mathrm{s}^{-1})$	265 ± 9	306 ± 9	336 ± 75	375^{+30}_{-300}	364 ± 46	345 ± 110	278

Two-body currents increase the rate by ~15%. Percent effects from 10% change in the axial mass

Addressing DUNE's physics

DUNE will be sensitive to a broad range of energies, characterized by different reaction mechanisms involving both nucleon and nuclear dynamics;

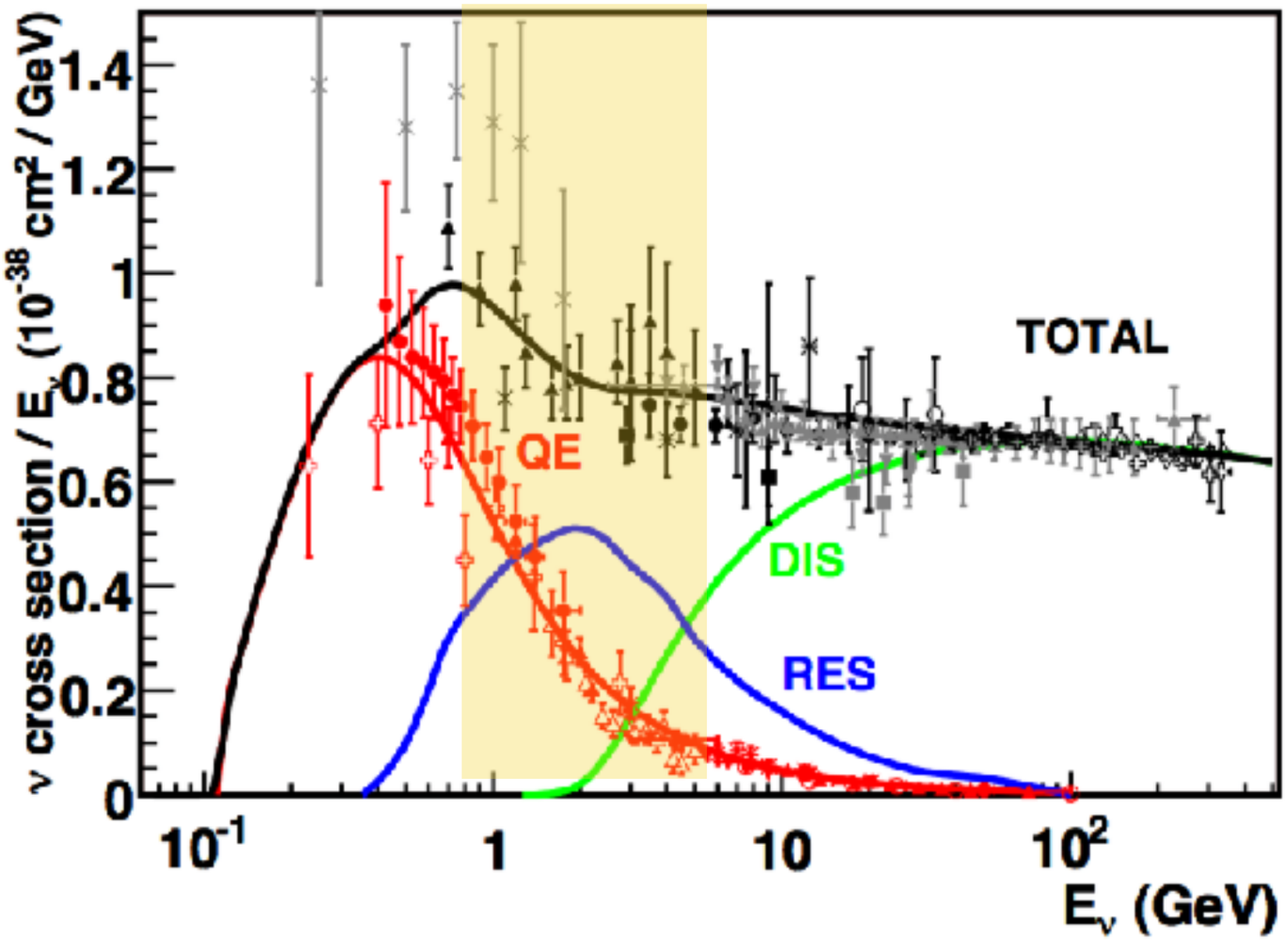

- Include fully relativistic (one- and two-body) currents and fully relativistic kinematics
- Resonance production and DIS scattering play an important role
- Keep a realistic description of the nuclear ground state

“Standard” factorization scheme

At **large momentum transfer**, scattering off a nuclear target reduces to the sum of scattering processes involving **individual bound nucleons**

$$J^\mu \to \sum_i j_i^\mu \qquad |\psi_f^A\rangle \to |p\rangle \otimes |\psi_f^{A-1}\rangle \qquad E_f = E_f^{A-1} + e(\mathbf{p})$$

The **incoherent contribution** of the one-body response reads

$$R_{\alpha\beta} \simeq \int \frac{d^3k}{(2\pi)^3} dE P_h(\mathbf{k}, E) \sum_i \langle k|{j_\alpha^i}^\dagger|k+q\rangle\langle k+q|j_\beta^i|k\rangle \delta(\omega + E - e(\mathbf{k}+\mathbf{q}))$$

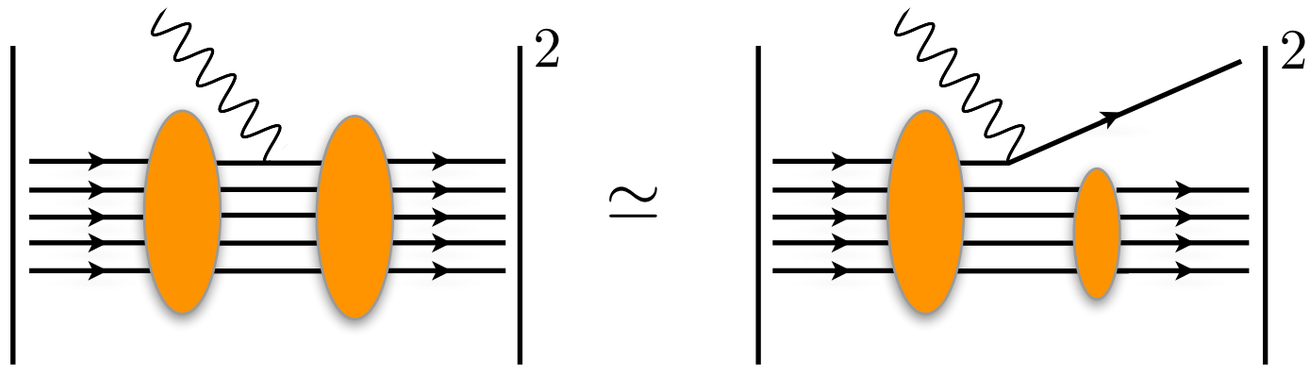

Excitations of the A-1 final state with **two nucleons in the continuum** are included

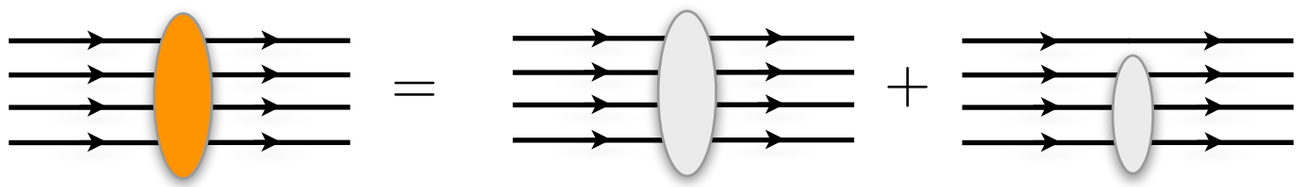

“Extended” factorization scheme

Using relativistic MEC requires **extending the factorization scheme** to two-nucleon emissions

$$|\Psi_f^A\rangle \rightarrow |p_1 p_2\rangle \otimes |\Psi_f^{A-2}\rangle$$

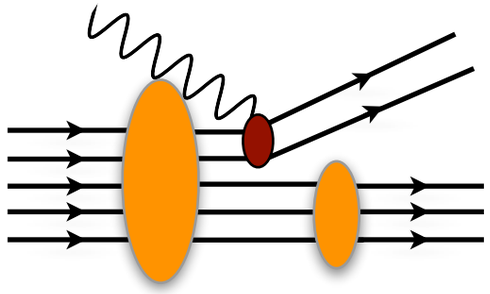

We compute electron and neutrino inclusive cross sections using CBF and SCGF spectral functions

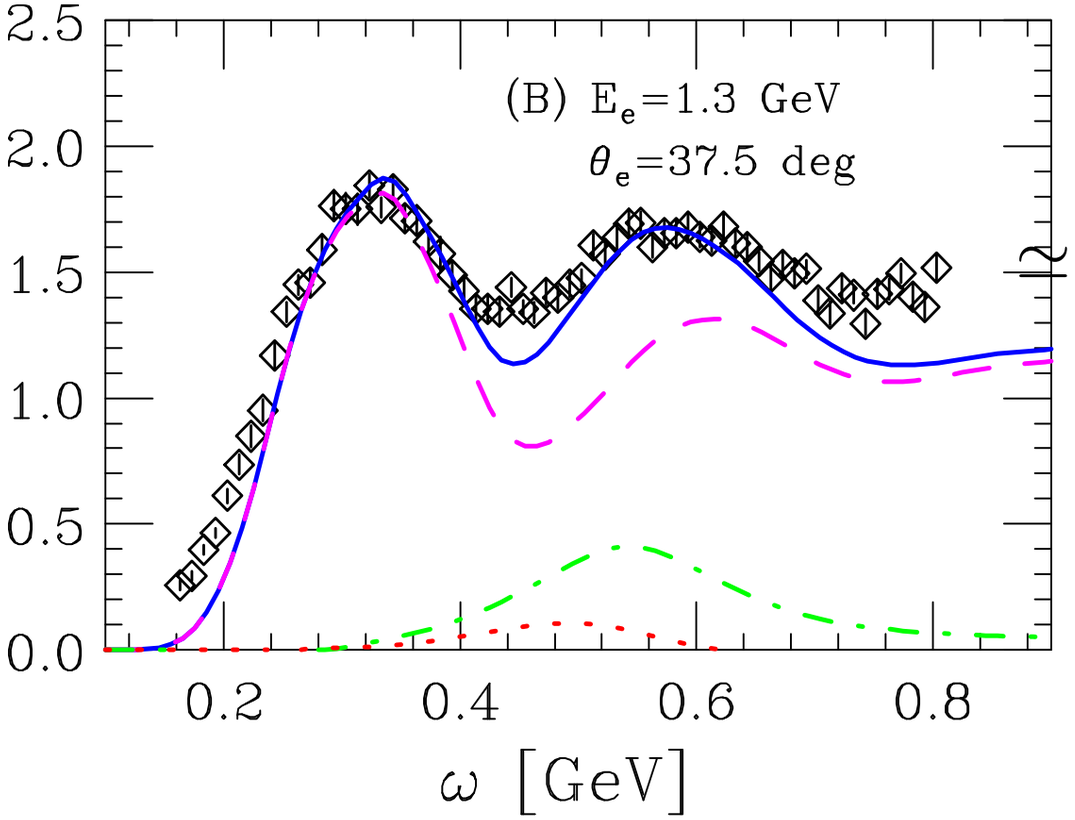

N. Rocco, et al. PRL. **116** 192501 (2016)

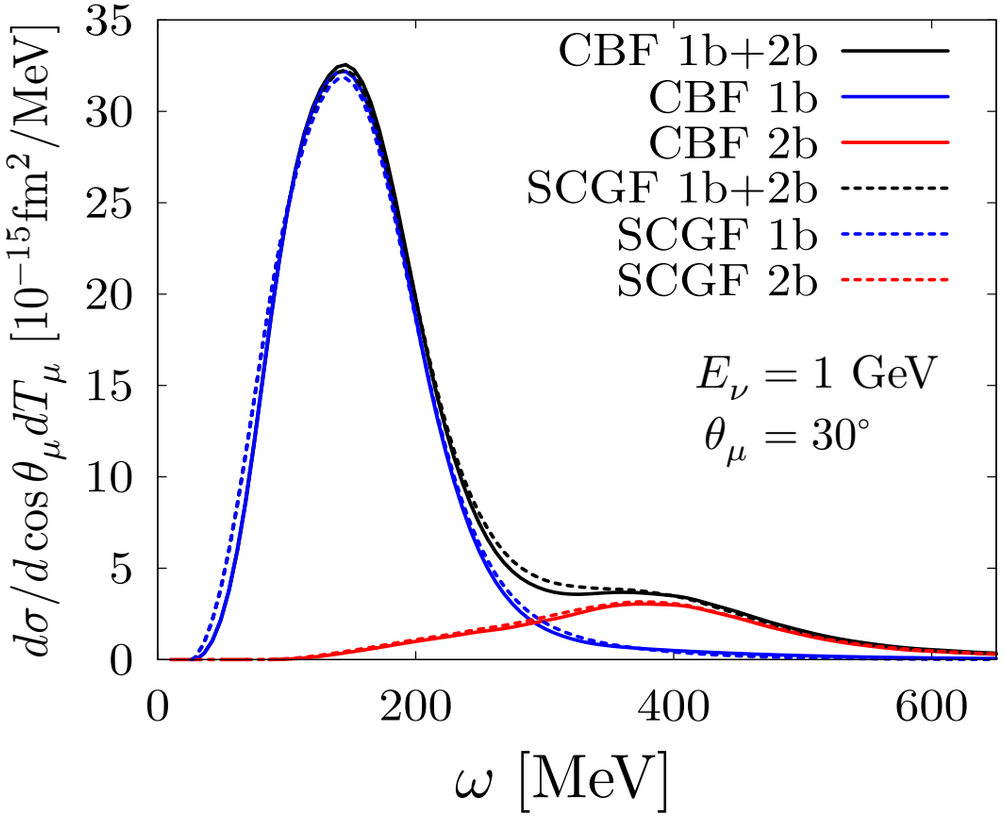

N. Rocco, et al. PRC **99** 025502 (2019)

“Extended” factorization scheme

The factorization scheme can be **further extended** to include real pions in the final state

$$|\Psi_f^A\rangle \rightarrow |p_1, p_\pi\rangle \otimes |\Psi_f^{A-1}\rangle$$

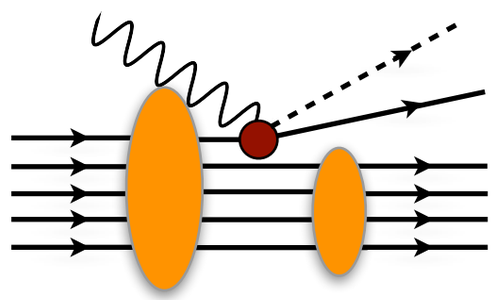

The DCC model, suitable to accurately describe single-nucleon pion-production, is folded with a realistic spectral function

The inclusion of pion production mechanism is essential to reproduce data in the resonance production region

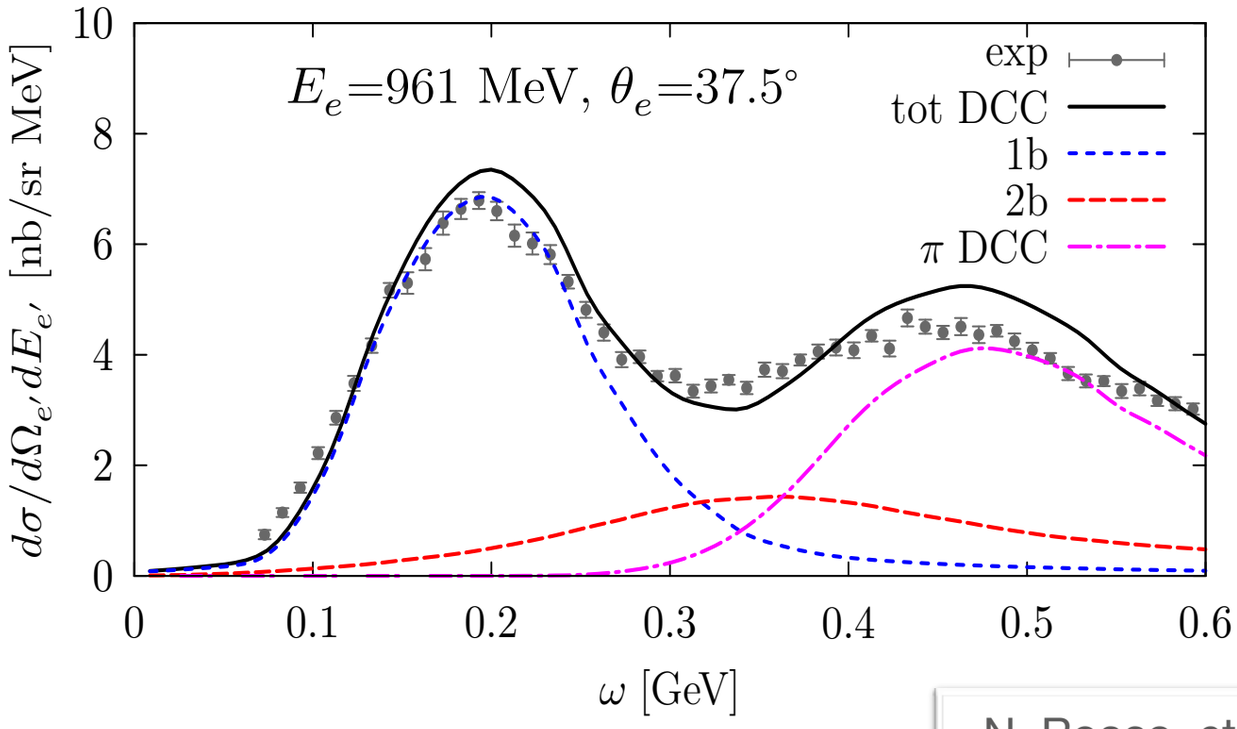

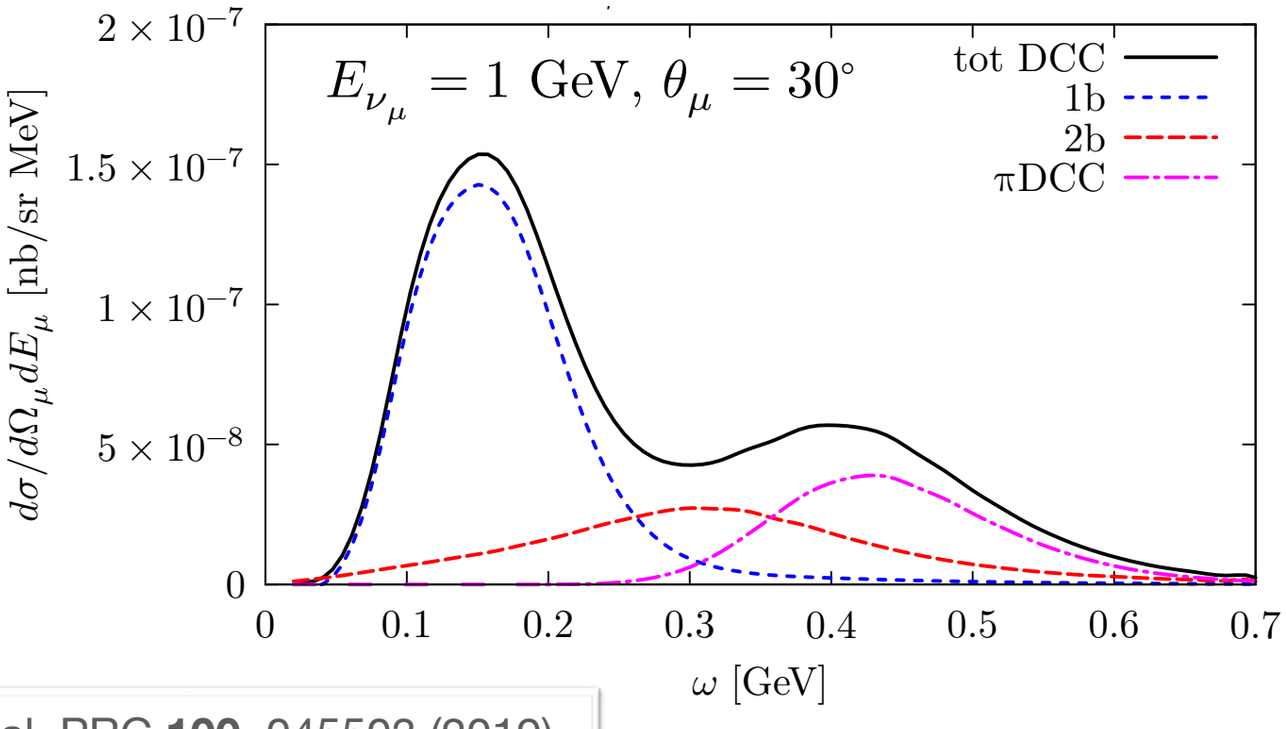

N. Rocco, et al. PRC **100**, 045503 (2019)

Summary and outlook

Lepton-nucleus scattering from quantum Monte Carlo

- ^{12}C electromagnetic responses in good agreement with experiments
- Two-body currents enhance electromagnetic, neutral- and charged-current responses
- Good agreement with MiniBooNE and T2K inclusive data → **First fully ab-initio results!**
- Total muon capture rate in ^{4}He agrees with available data → **Need new experiments!**
- Exploit deep-learning techniques to improve the accuracy of the inversion

Extended factorization scheme

- Two-body currents and pion-production mechanisms are essential to reproduce electron-scattering data
- Cluster expansion formalism to improve treatment of FSI and interference

Some developments

Use **Deep Learning algorithms** to improve the inversion of the Euclidean response

We train the neural network providing a large number (200,000) of templates for the response functions and the corresponding set of Euclidean responses

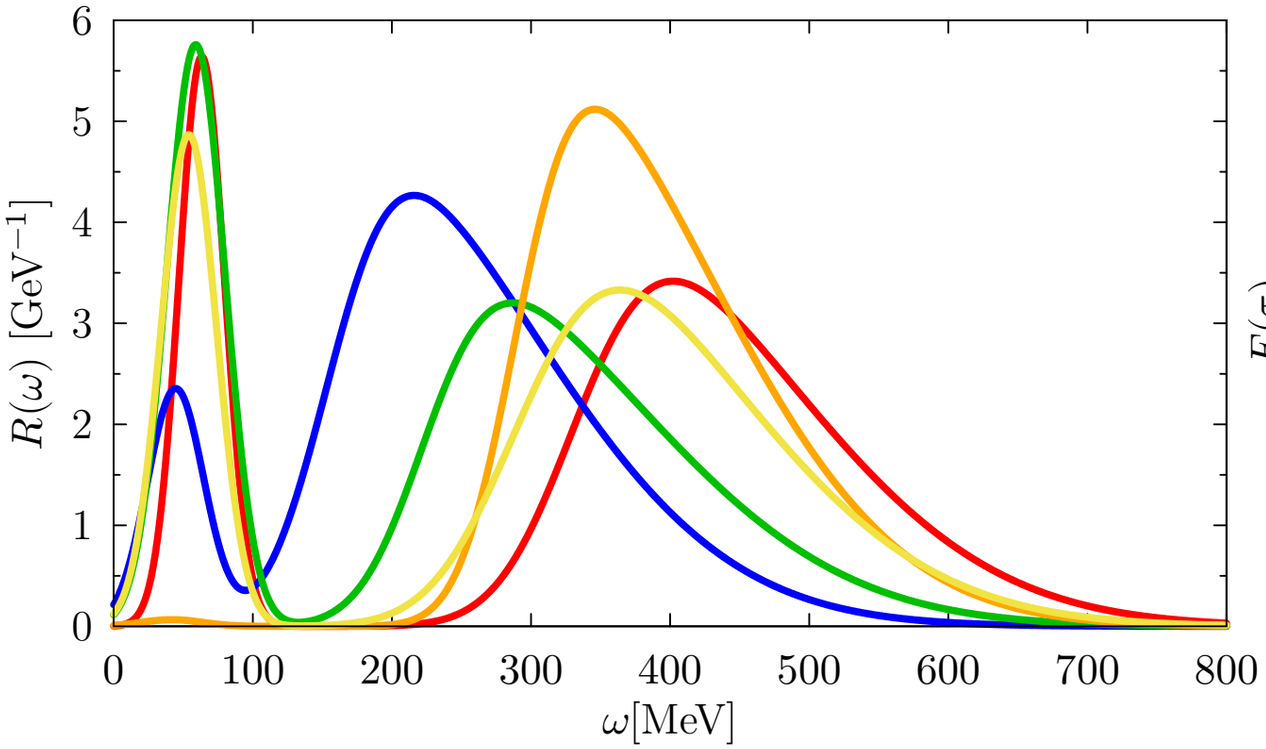

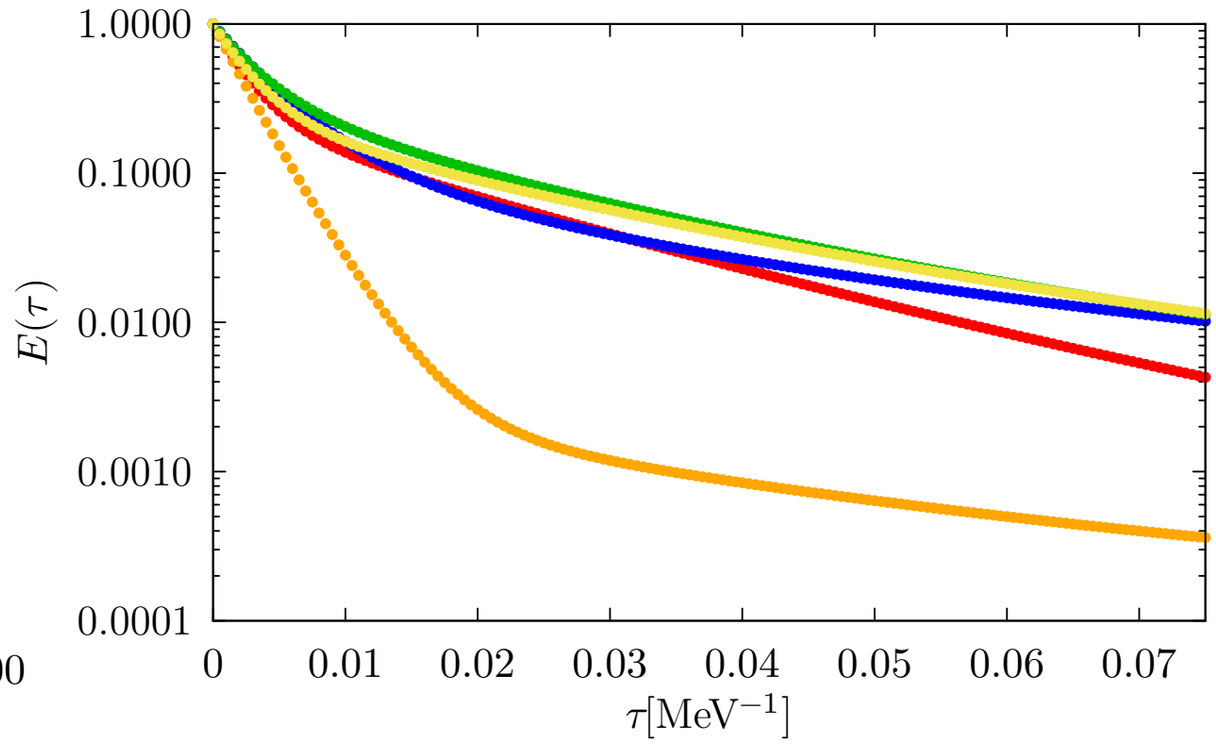

Short-term goal: resolve coherent peak at low energy transfer, reduce the computational cost

Long-term goal: achieve accurate inversions with robust error propagation

Some developments

Preliminary results are encouraging for both single- and two-peaks responses

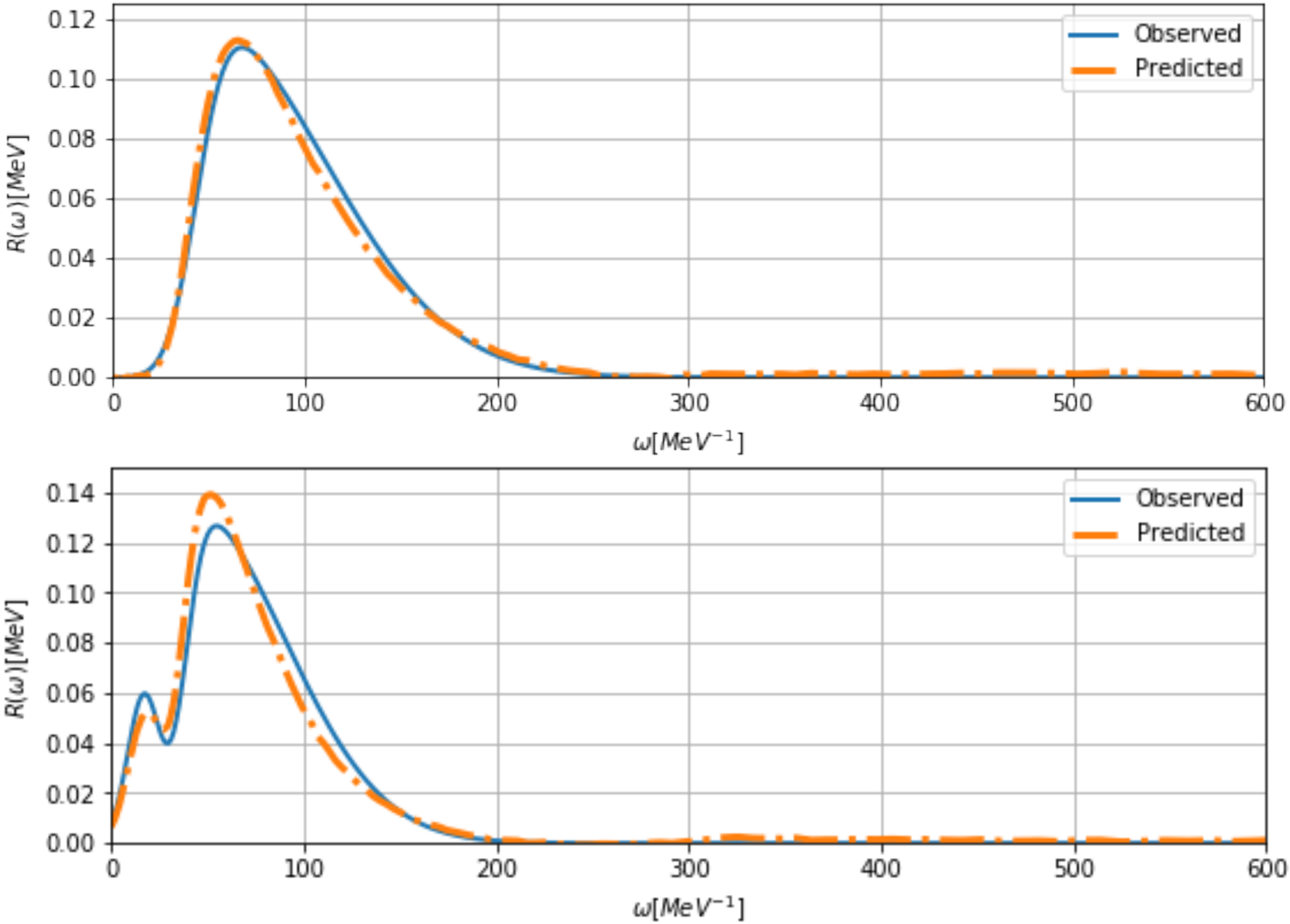

Thank you